

Nature-inspired hierarchical materials

Original

Nature-inspired hierarchical materials / Fu, Q.; Baino, F.; Saiz, E.; Bai, H.; Mauro, J. C.. - In: JOURNAL OF THE AMERICAN CERAMIC SOCIETY. - ISSN 0002-7820. - 108:11(2025). [10.1111/jace.70156]

Availability:

This version is available at: 11583/3005909 since: 2025-12-16T11:30:08Z

Publisher:

John Wiley and Sons

Published

DOI:10.1111/jace.70156

Terms of use:

This article is made available under terms and conditions as specified in the corresponding bibliographic description in the repository

Publisher copyright

(Article begins on next page)

FEATURE ARTICLE

Nature-inspired hierarchical materials

Qiang Fu¹  | Francesco Baino²  | Eduardo Saiz³ | Hao Bai⁴  |
John C. Mauro⁵ 

¹Science & Technology Division, Corning Incorporated, Corning, New York, USA

²Institute of Materials Physics and Engineering, Applied Science and Technology Department, Politecnico di Torino, Torino, Italy

³Centre for Advanced Structural Materials, Department of Materials, Imperial College London, London, UK

⁴State Key Laboratory of Chemical Engineering, College of Chemical and Biological Engineering, Zhejiang University, Hangzhou, China

⁵Department of Materials Science and Engineering, The Pennsylvania State University, University Park, Pennsylvania, USA

Correspondence

Qiang Fu, Science & Technology Division, Corning Incorporated, Corning NY 14831, USA.

Email: fuq2@corning.com

Abstract

Nature serves as an exemplary model for materials science, demonstrating how organisms develop their hierarchical structures and multifunctional properties with limited, locally available materials through evolution. This approach addresses complex design challenges while enabling a sustainable, recycling biological cycle. This article explores the intersection of materials science and natural organisms, focusing on bone, nacre, sea sponge, and spider silk as key examples. These natural materials achieve exceptional mechanical properties, such as strength, toughness, and adaptability, using minimal resources under ambient conditions. Their intricate architecture and design principles have inspired the development of advanced, sustainable materials for various applications, as illustrated in several case studies in this article. In healthcare, bioinspired materials are transforming tissue engineering and regenerative medicine by creating porous scaffolds that replicate the complexity of natural bone tissues and ultimately enhance bone regeneration. In energy storage, incorporating hierarchical structures into lithium-ion battery electrodes improves electron conductivity and ion transport, resulting in more efficient and durable solutions. For sustainability, innovations in engineered “living” materials, such as microbial-induced carbonate precipitation and self-healing concrete, and in spider silk-inspired water collection systems, contribute to more resilient infrastructure and sustainable water sources. Furthermore, the role of artificial intelligence and machine learning in predicting three-dimensional protein structures and facilitating the design of novel bioinspired materials is discussed. This review serves as a foundation for further exploration and refinement, aiming to shed new light on transformative innovations enabled by nature-inspired material design.

KEYWORDS

artificial intelligence, all-solid state battery, bone, bioinspired materials, extensibility, hierarchical structure, healthcare, lithium-ion battery, machine learning, nacre, porous scaffolds, sustainability, self-healing, sea sponge, spider silk, strength, toughness, tissue engineering, water collection

This is an open access article under the terms of the [Creative Commons Attribution](https://creativecommons.org/licenses/by/4.0/) License, which permits use, distribution and reproduction in any medium, provided the original work is properly cited.

© 2025 The Author(s). *Journal of the American Ceramic Society* published by Wiley Periodicals LLC on behalf of American Ceramic Society.

1 | INTRODUCTION

Nature serves as an exemplary model for materials science, offering profound insights through the hierarchical structures of organisms that address complex design challenges.^{1–4} Natural biological structures are typically assembled under mild conditions (ambient temperature and pressure in an aqueous system),^{5–7} using limited resources immediately available in their environment, including elements like carbon, nitrogen, calcium, hydrogen, oxygen, silicon, and phosphorus.⁸ In addition, they are primarily built from three basic constituents: minerals, proteins, and sugars (Figure 1),⁵ which are considered much weaker than engineering materials.^{5–9}

Despite being limited in material selection, biological systems use hierarchical structuring to achieve exceptional mechanical, thermal, electrical, and optical properties with minimal energy and resources.⁵ By organizing materials across scales—from molecular to macroscopic—organisms enhance strength, flexibility, and durability beyond the capabilities of the raw materials.^{1,5} Additionally, the uniformity and limited diversity of base materials, mainly proteins and polysaccharides, facilitate easy degradation and reuse via enzymes, a natural sustainable approach with fewer materials tailored for specific functions.^{5,10} Natural organisms share several unique features,^{8,11} including (1) *self-assembly* by constructing from the bottom up; (2) *hierarchical structure* at multiple levels of scales; (3) “*simplicity*” in synthesis in an aqueous environment and at ambient temperature; (4) *multifunctionality* within one system; and (5) *self-healing* to adapt to the changing environment.

For decades, the intriguing properties in natural organisms, such as hierarchical organization, unique surface functionality, and high adaptability, as those shown in Figure 2, have inspired the design of innovative materials for advanced, sustainable, and high-performance solutions to human challenges.^{1,8,12,13} To provide a glimpse of nature-inspired materials design, three types of material and system innovations enabled through the biomimeticism of natural organisms are listed below:

1. *Hierarchical structure*: Many natural organisms and tissues (such as nacre, bone, teeth, fish scales, lobster cuticle, wood, bamboo, spider silk, and glass sponge) are built in a hierarchical way at multiple length scales.^{1,7,3} Among them, bone, nacre, and spider silk are the most investigated due to their unique structure and properties, such as the strong, porous structure in human bone; the tough, layered structure in nacre; and the high strength and elasticity in spider silk.^{1,7,3} Meanwhile, the hierarchical structure in glass sponges has received increasing attention due to its unique ductile failure mode.^{14–16} Inspirations from them have resulted in the development of porous tissue engineering scaffolds,^{17–23} impact-resistant composites,^{13,24–26} and lightweight fibers in medical devices.^{27–31}
2. *Smart surface*: The wetting and self-cleaning properties of biological matter (such as lotus leaf, rice leaf, butterfly wing, fish scale, and shark skin),^{32–34} as shown in Figure 2A–C, resulting from nano-and-micrometer-scale roughness, have driven the design of controlled surface topographies for practical applications.^{35,36} For example, the hierarchical structure of the superhydrophobic lotus leaf has inspired the design of micropatterned surfaces on silicon wafers and metal foils for self-cleaning,^{36–39} and the fabrication of superhydrophobic nanoporous silica thin films on glass,^{40,41} among others.
3. *Adaptive functionality*: Through controlling the sophisticated architecture of their pigment cells, both chameleons and cephalopods exhibit remarkable ability to manipulate their skin color and texture for camouflage, communication, and thermoregulation.^{8,42–44} As an example, chameleons have an evolutionary adaptation involving two distinct layers of iridophores. The upper multilayer (S-iridophores) actively adjusts the spacing of guanine nanocrystals in a triangular lattice, enabling rapid changes in structural color for camouflage and display, as shown in Figure 2D.⁴² The deeper layer of cells (D-iridophores) reflects sunlight, particularly in the near-infrared range, helping manage the thermal effects of intense solar radiation while contributing to camouflage and display capabilities.⁴² Learning from the color-changing capability and associated functions has inspired the engineering of a variety of artificial optoelectronic devices such as stretchable electronic skin^{45–47} and soft robots.^{48,49}

Several textbooks and review articles on the structure and properties of biological materials can be found in literature.^{1,5,7,8,11,3,50} Consequently, this article does not aim to provide an exhaustive review of these topics. Instead, it offers a perspective on the intersection of materials science and natural organisms, emphasizing the use of biological insights to design novel materials with hierarchical structures to address significant challenges in healthcare, energy, sustainable development, and beyond.

This article examines the design principles of four notable examples of hierarchical structures: bone, nacre and sea sponge as mineralized (“hard”) ceramic composites, and spider silk as a non-mineralized (“soft”) polymer composite. It explores the diverse applications of nature-inspired materials and discusses the potential of bioinspired materials design enhanced by artificial intelligence (AI). The article is organized into five sections.

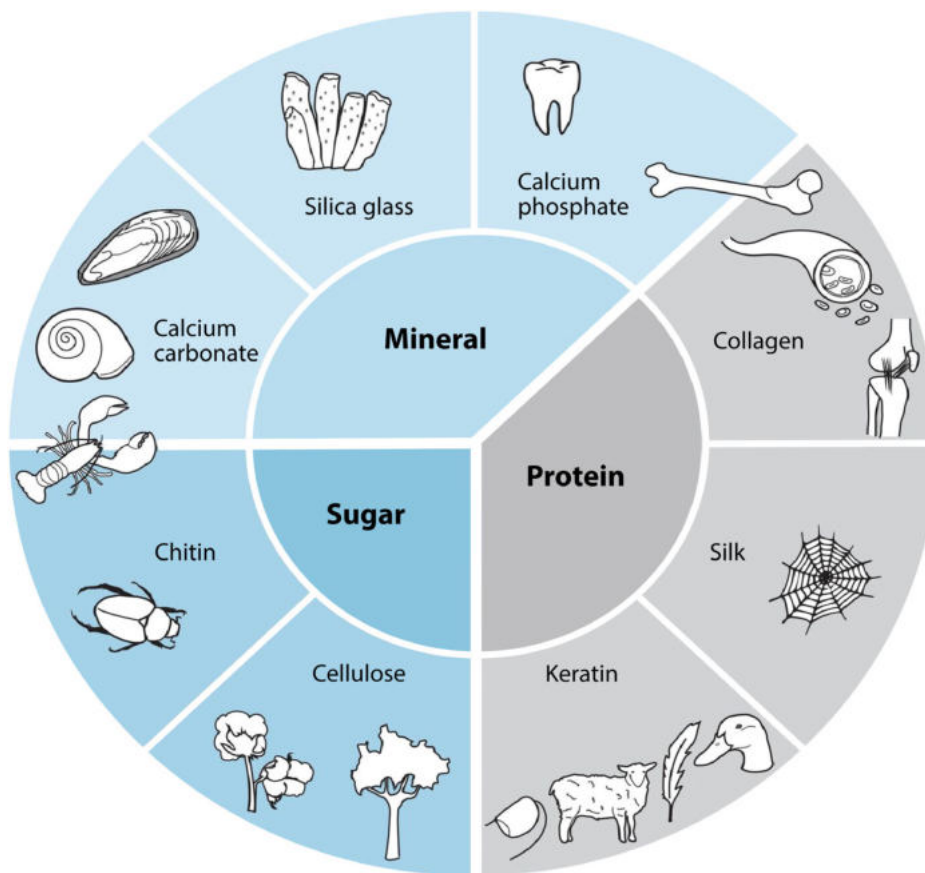


FIGURE 1 Biological materials are built with a limited number of building blocks, based on polysaccharides, proteins, and minerals. A diversity of structures leads to a diversity of functions in tooth, bone, artery wall, tendon, spider web, beak, feather, wool, fingernail, tree, cotton, beetle carapace, lobster shell, snail shell, mussel shell, and the skeleton of the glass sponge (clockwise from top). *Source:* Reprinted with permission from Ref. [5], American Association for the Advancement of Science (AAAS).

Section 2 provides a brief description of the hierarchical structure and mechanical properties of the four example biological materials mentioned above (bone, nacre, sea sponge, and spider silk). Section 3 focuses on bioinspired materials design for applications in healthcare, energy, and sustainability. Section 4 discusses the use of AI to harvest the inspiration from natural materials to guide the design of novel synthetic materials. We conclude with recommendations for future research directions in the development of novel materials inspired by natural organisms.

2 | NATURAL HIERARCHICAL ORGANISMS

Natural materials excel at integrating multiple functions—biological, mechanical, and adaptive—within a single system. This versatility is evident in the Ashby plot shown in Figure 3, which compares the mechanical properties (toughness vs. Young's modulus) of natural and synthetic materials across different material families.^{1,9,51} Here, toughness refers to a material's ability to resist frac-

ture and is quantified by the energy required to cause it to break. It can also be assessed using fracture mechanics approaches, which determine the critical values of crack-driving forces—such as stress intensity (K in $\text{MPa m}^{0.5}$), strain energy release rate (G in J m^{-2} , or MJ m^{-3}), or the nonlinear elastic J -integral—needed to initiate or propagate an existing crack.⁵²

Although natural hierarchical structures, such as bone, nacre, and dentin, generally exhibit lower strength values compared to engineering ceramics and metals, spider silk is an exception due to its excellent strength and toughness. Unlike most synthetic materials, natural organisms construct their structures from a limited array of naturally available ingredients—proteins, polysaccharides, silicon oxide, calcium carbonate, calcium phosphate, and minimal metals—under ambient temperature and pressure conditions. Despite these constraints, natural organisms achieve remarkable toughness, far exceeding their composition and their homogeneous mixture,¹ by combining multiple toughening mechanisms at different length scales through their hierarchical structure. It is also worth noting that bioinspired hierarchically structured composites have

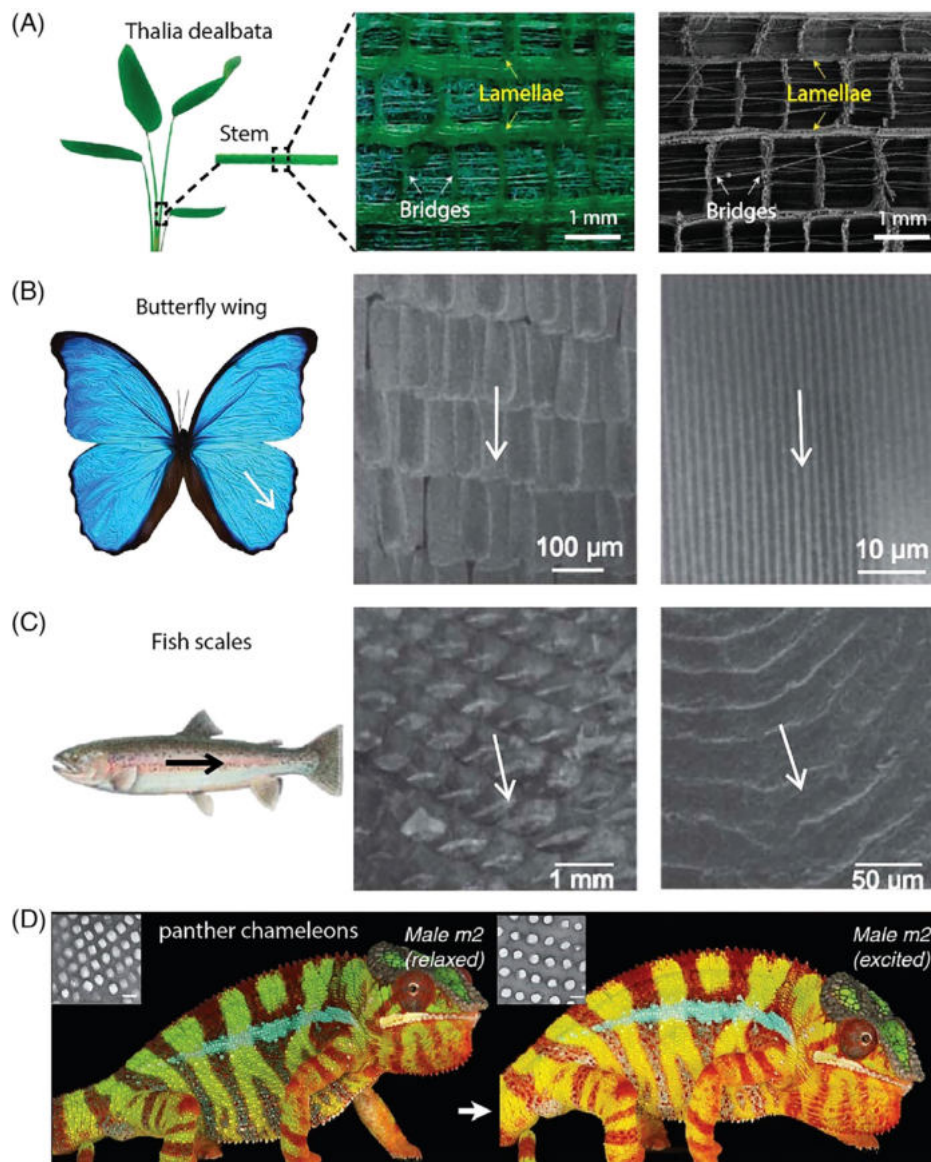


FIGURE 2 Hierarchical design in biological materials: (A) optical and scanning electron microscope (SEM) images of the multiscale porous structure of a *Thalia dealbata* stem; (B) digital photo and SEM images of butterfly wings; (C) digital photo and SEM images of fish scales; (D) reversible color change for a male panther chameleon from relaxation to excitation (white arrows). Inset TEM images of the lattice of guanine nanocrystals in S-iridophores from the same individual in a relaxed and excited state (two biopsies separated by a distance <1 cm, scale bar, 200 nm). *Source:* (A) Reprinted with permission from Ref. [33], John Wiley & Sons, Inc. (B) Reprinted with permission from Ref. [32], Royal Society of Chemistry. (C) Reprinted with permission from Ref. [32], Royal Society of Chemistry. (D) Reprinted with permission from Ref. [42] Springer Nature.

demonstrated the highest combinations of toughness and stiffness.⁹

Among various natural organisms, bone, nacre, and sea sponge stand out as prime examples of ceramic composite materials that combine strength and toughness to achieve high damage tolerance. Similarly, spider silk, a polymer composite, exhibits mechanical properties superior to almost all natural or man-made materials.^{1,8,9} Comprehensive reviews detailing the structure, strength, and toughening mechanisms of these four hierarchical materi-

als are available in several review articles and books.^{1,7-9,53} Therefore, a brief overview, complemented by schematic illustrations, is presented here to elucidate their general design principles.

2.1 | Bone

Bone comes in a variety of shapes and sizes, which corresponds to their different functions including

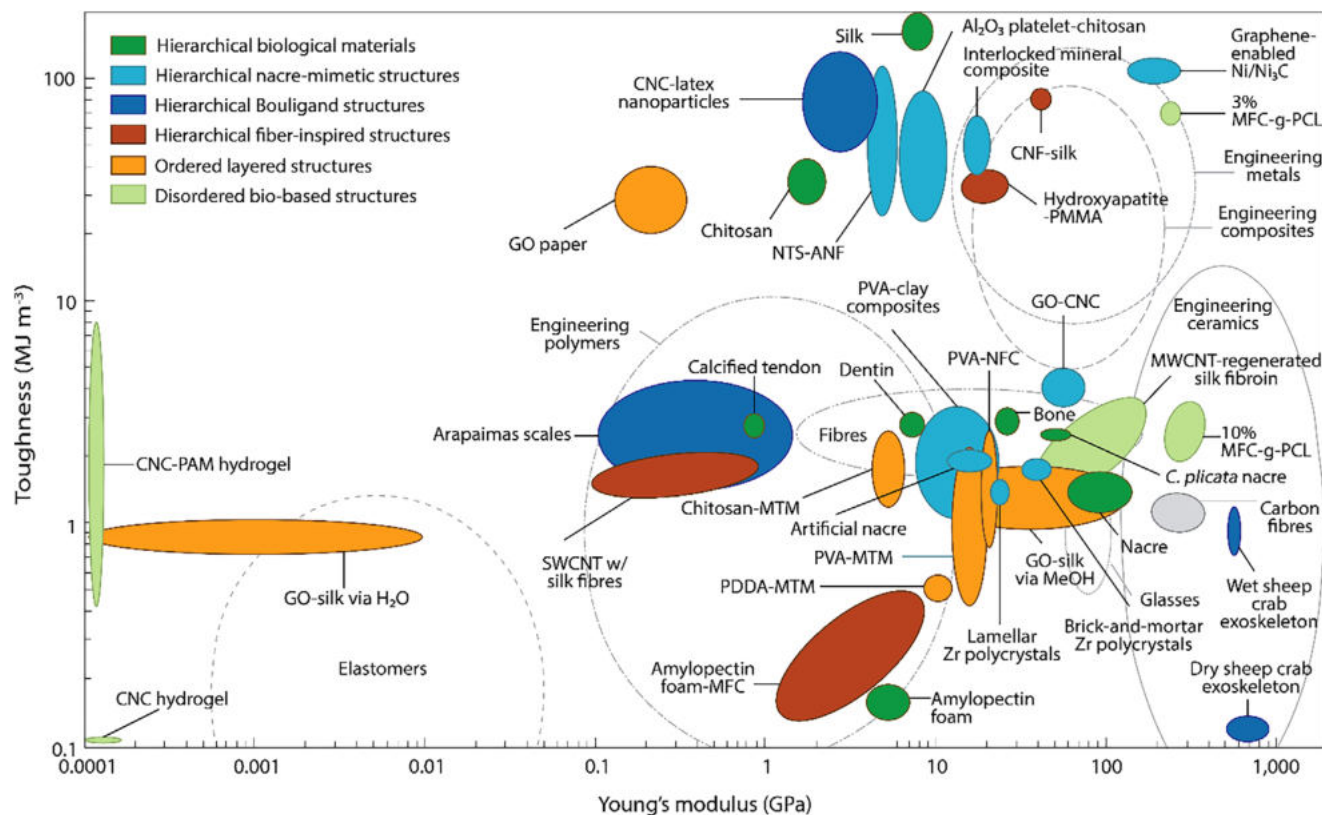


FIGURE 3 Ashby material–property chart, comparing the toughness (energy to failure) versus Young’s modulus for various hierarchical biological materials, bioinspired structures, and traditional engineering materials. Hierarchically structured composites achieve the highest combinations of toughness and stiffness. Composites that include biological fibrous components are among the best-performing materials. ANF, aramid nanofiber; CNC, cellulose nanocrystal; GO, graphene oxide; MFC, microfibrillated cellulose; MTM, montmorillonite; MWCNT, multiple-walled carbon nanotube; NFC, nanofibrillated cellulose; PCL, polycaprolactone; PVA, poly(vinyl alcohol); SWCNT, single-walled carbon nanotube. *Source:* Reprinted with permission from Ref. [9], Springer Nature.

protection and structural support without compromising the requirements of mobility.⁷ A typical long bone in the limbs comprises two types of bones, each with a different structural organization: cortical bone, also referred to as compact bone, and trabecular bone, also referred to as cancellous or spongy bone.⁵⁴ Figure 4 illustrates the structure of a long bone, highlighting the dense surface cortical bone and the inner porous trabecular bone.

Structurally, bone is a composite material composed of several key components. It consists of collagen fibrils (35 wt% based on dry bone, approximately 300 nm long and 1.5 nm in diameter) derived from Type-I collagen molecules, which contribute to its flexibility and toughness. Additionally, bone contains hydroxyapatite (HA, $\text{Ca}_{10}(\text{PO}_4)_6(\text{OH})_2$, 65 wt%) nanocrystals that are plate-shaped (50 nm \times 25 nm in size, with a thickness of 1.5–4 nm), providing structural reinforcement, stiffness, and mineral homeostasis. Other non-collagenous proteins are also present to support cellular functions.^{54,55}

The architecture of bone, albeit complex, can be described across seven hierarchical levels of organization.

These levels include HA crystals and mineralized collagen fibrils at the nanometer scale; fibril arrays and their corresponding patterns, and osteons at the micrometer scale; and the overall structure of cortical and trabecular bone to form a whole bone at the macroscopic scale.^{56,57}

Cortical bone exhibits notable mechanical properties, with a compressive strength ranging from 100 to 150 MPa in the longitudinal direction and a flexural strength between 135 and 193 MPa. The fracture toughness (K_{IC}) of cortical bone ranges from 2 to 12 $\text{MPa m}^{0.5}$, which is up to an order of magnitude higher than that of its constituent mineral, HA. Table 1 presents a summary of the mechanical properties of bone and its constituent mineral.

The high fracture toughness of cortical bone is attributed to a combination of intrinsic and extrinsic toughening mechanisms. Intrinsic toughness arises from plasticity mechanisms at the sub-micrometer scale, which involve the molecular uncoiling of collagen molecules, sliding of mineralized collagen fibrils, and microcracking. Extrinsic toughening mechanisms operate over length scales of approximately

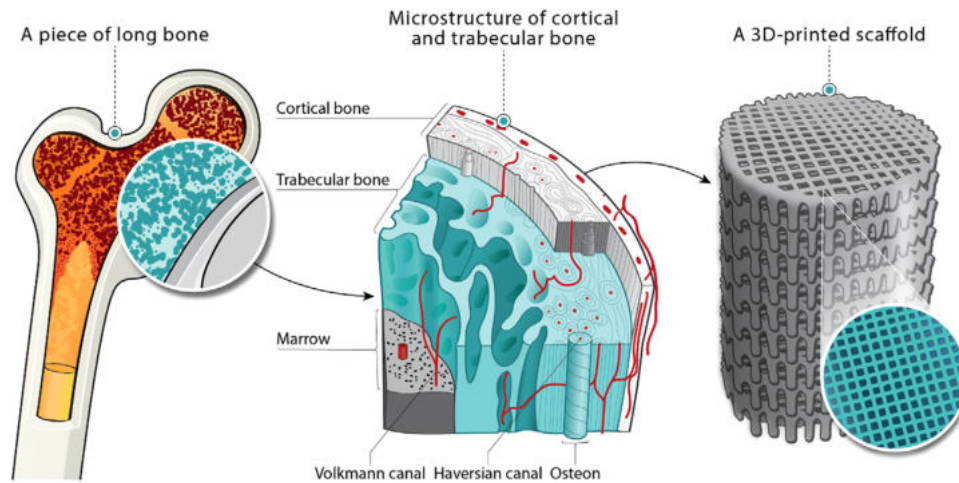


FIGURE 4 An illustration showing the bone structure and a bone-inspired, porous, three-dimensional (3D)-printed scaffold. Left, internal structure of a human long bone; middle, a magnified cross section of the interior; right, a bone-inspired 3D-printed scaffold with periodic porosity.

TABLE 1 Mechanical properties of bone and its constituent mineral hydroxyapatite.

Materials	Compressive strength (MPa)	Flexural strength (MPa)	Tensile strength (MPa)	Young's modulus (GPa)	Fracture toughness ($\text{MPa m}^{0.5}$)	Porosity (%)
Cortical bone ^{53,58–63}	100–150	135–193	50–151	10–20	2–12	5–10
Trabecular bone ^{53,58,64,65}	2–12	N/A	1–5	0.1–5	0.1–0.8	50–90
Sintered hydroxyapatite ^{66,67}	500–1000	115–200	38–300	80–130	0.6–1.0	<5

1–100 μm and include crack deflection/twisting and crack bridging.^{57,68}

2.2 | Nacre

Although bone achieves its exceptional mechanical properties through a complex structure, nacre (the interior portion of the abalone shell) attains similar performance through a relatively simplistic architecture. Figure 5 schematically illustrates the typical “brick-and-mortar” structure found in abalone nacre, which serves as the primary means of protection for the soft body inside the shell.

In nacre, the mineral phase (“brick”) consists of layered hexagonal aragonite (CaCO_3) platelets, approximately 0.2–0.9 μm thick with a diameter of 5–9 μm , which accounts for 95 vol% of the composite. These inorganic platelets are sandwiched between thin (10–50 nm thick) sheets of a protein–polysaccharide organic matrix (“mortar”),⁸ which plays a crucial role in controlling the thickness of the aragonite crystals and in the mechanical design of nacre.^{7,8} Although the ceramic phase (calcium carbonate) is stiff and hard, it is brittle without a means to dissipate strain.

In nacre, energy dissipation is achieved through inelastic deformation produced by the organic phase.^{7,8}

As a result of its hierarchical structure, nacre exhibits a toughness (in terms of energy to failure) of about 3000 times higher than the materials it is made of.⁶⁹ It can undergo up to 1% tensile strain before failure,⁷⁰ and its fracture toughness (K_{IC}), in the range of 4–10 $\text{MPa m}^{0.5}$, is up to 40 times that of aragonite 0.25 $\text{MPa m}^{0.5}$.⁷¹ Given its unique “brick-and-mortar” structure and the resulting damage mechanisms, nacre exhibits a high orientation dependence of strength.⁷² The mechanical properties of nacre tested with loading parallel to the major plane of platelets and its mineral constituent aragonite are summarized in Table 2.

The exceptional mechanical properties of nacre are enabled through a series of toughening mechanisms resulting from its unique “brick-and-mortar” structure.^{1,8,69,70} Similar to bone, the toughening of nacre is largely extrinsic.¹ The principal toughening mechanisms in nacre include the following:^{1,7,8,12,24,37,69–71} (1) crack deflection along the inter-platelet organic phase; (2) “pull-out” of the aragonite platelets; (3) bridging by mineral and organic matrix; and (4) interlocking of platelets. The organic matrix plays a crucial role in toughening nacre by effectively dissipating energy as cracks open through bridging

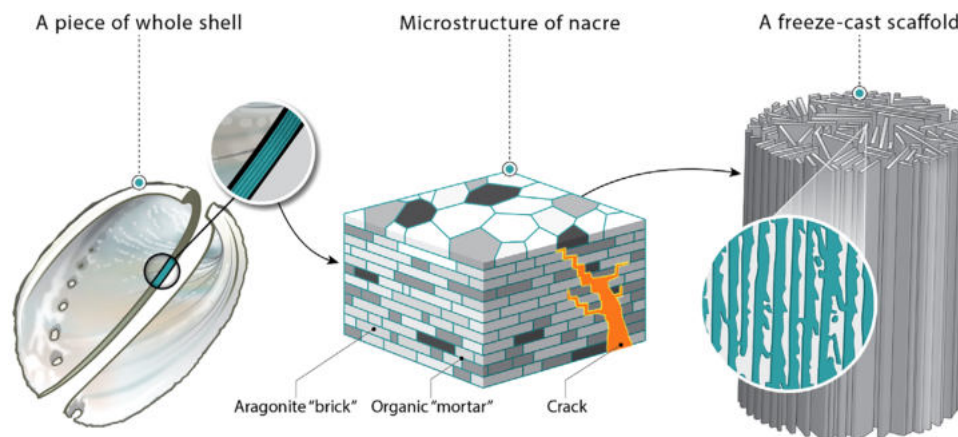


FIGURE 5 An illustration showing the nacre structure and a nacre-inspired, porous freeze-cast scaffold. Left, a piece of shell; middle, a magnified cross section to illustrate the “brick-and-mortar” structure in nacre and the crack deflection, one of the prevailing toughening mechanisms, resulting from its unique structure; right, a nacre-inspired freeze-cast scaffold with oriented lamellar porosity.

TABLE 2 Mechanical properties of nacre and its constituent mineral, aragonite.

Materials	Compressive strength (MPa)	Flexural strength (MPa)	Tensile strength (MPa)	Young's modulus (GPa)	Fracture toughness (MPa m ^{0.5})
Nacre ^{a69,71–73} (abalone shell)	235–540	165–205	35–140	50–72	4–10
Aragonite ^{1,70,72,74–76}	N/A	N/A	160	82–144	0.25

^aData are limited to wet or fresh samples and loading parallel to the major plane of the aragonite platelet in nacre.

between the platelets and the unfolding of its protein structure.

2.3 | Sea sponge

Sea sponges exhibit a highly hierarchical structural complexity and are widely recognized for their ability to construct exceptional skeletons using amorphous hydrated silica.^{8,50} Their glass-like skeletal components, known as spicules, are precisely arranged in a square grid pattern reinforced by two intersecting sets of paired diagonal supports. This unique configuration results in a checkerboard-like structure composed of alternating open and closed cells,¹⁴ as shown in Figure 6A–C. Each spicule is composed of a protein-based central core encased in concentric layers of compacted silica nanoparticles, interspersed with thin organic interlayers (silicatein),^{15,16} as depicted in Figure 6D–G. This “onion skin” structure enhances crack resistance and significantly improves flexural strength, making it four times stronger than monolithic silica.⁷⁷ The mechanical performance of sea sponges is largely influenced by the striated layers, which provide crack deflection and energy absorption at the interfaces.^{77,78}

Drawing inspiration from the hierarchical structure of sea sponges, mechanically robust lattices produced via three-dimensional (3D) printing have demonstrated exceptional buckling resistance for a given material volume by incorporating the sponge’s diagonal reinforcement strategy,¹⁴ as illustrated in Figure 6H–J. Additionally, hierarchical lattice metamaterial with modified face-centered cubic cells achieves controllable deformation patterns by combining bionic features such as double diagonal reinforcement with hierarchical circular modifications,⁷⁹ suggesting their significant potential for enhancing material efficiency in contemporary infrastructural applications.

2.4 | Spider silk

Although bone, nacre, and sea sponge are biological tissues containing mineral components, spider silk represents a typical hierarchical polymer composite composed of organic proteins.^{8,80} Figure 7 schematically illustrates the sophisticated architecture of spider silk.

To the naked eye, an orb web appears uniform, but it is constructed from up to five different types of silk: (1) dragline silk, or major ampullate silk, which is used for

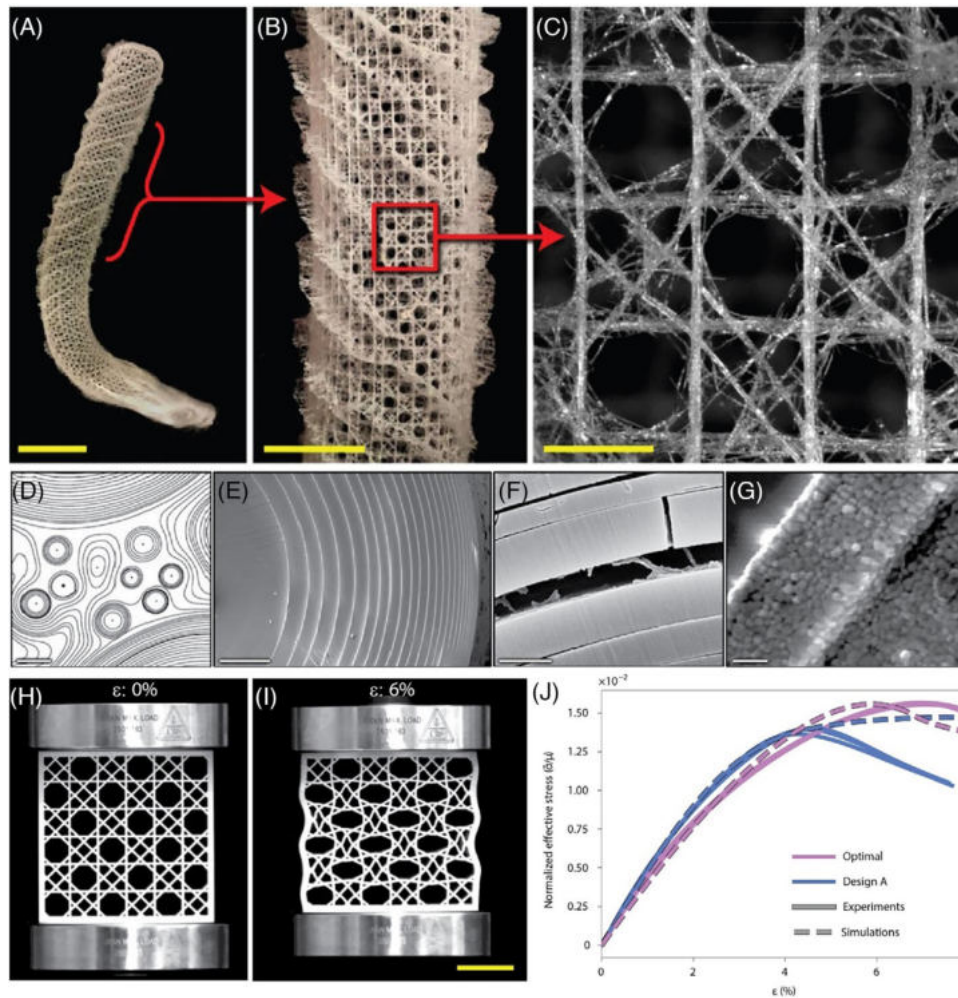


FIGURE 6 Progressively magnified views of the sponge's skeletal system, showing optical images of (A) the entire skeletal tube, (B) a magnified view of its highly regular lattice-like organization, and (C) its alternating arrangement of open and closed cells; and scanning electron microscopy (SEM) images of (D) contrast-enhanced image of a cross section through one of the spicular struts, revealing that they are composed of a wide range of different-sized spicules surrounded by a laminated silica matrix, (E) a cross section through a typical spicule in a strut, showing its characteristic "onion skin" laminated architecture, (F) a fractured spicule, revealing an organic interlayer, and (G) nanoparticulate nature in a bleached biosilica surface. In addition, sea sponge-inspired, three-dimensional (3D)-printed structures subjected to 0% applied strain (H) and 6% applied strain (I), and simulated and normalized experimental stress–strain curves for different structural designs (J). Scale bars: 4 cm (A); 2 cm (B); 2.5 mm (C); 10 μm (D); 5 μm (E); 1 μm (F); 500 nm (G); and 3 cm (I). Source: (A)–(C) and (H)–(J) were reprinted with permission from Ref. [14], Springer Nature. (D)–(G) were reprinted with permission from Ref. [15], American Association for the Advancement of Science (AAAS).

safety lines, web frames, and lifelines; (2) flagelliform silk, which forms the prey-catching spirals of the web; (3) aggregate silk, which secretes a glue to coat the spiral silk; (4) minor ampullate (Mi) silk, which provides reinforcement; and (5) piriform silk, which attaches draglines to substrates.^{8,80,81}

Spider silk is a remarkable material, exhibiting a combination of high tensile strength, extensibility, and toughness,⁸² surpassing even the strongest man-made materials (Table 3). Among the various types of spider silk, dragline and flagelliform silks are the most extensively studied due to their unique mechanical properties.⁸³

Dragline silk, in particular, has been found to possess a high strength exceeding 1 GPa.

Despite their varying mechanical properties, which depend on the application intended by the spider, all spider silk threads share a similar hierarchical structure at three different levels. On the molecular level (nanometer scale), crystalline β -sheets (comprising 10–15 vol%), made up of poly-(Gly-Ala) and poly-Ala repeats, are embedded in an amorphous protein matrix containing helical structures oriented along the fiber axis,^{80,81,83–86} as illustrated in Figure 7. The amorphous matrix, composed of the G-rich motifs of MaSp1 and the P-containing motifs

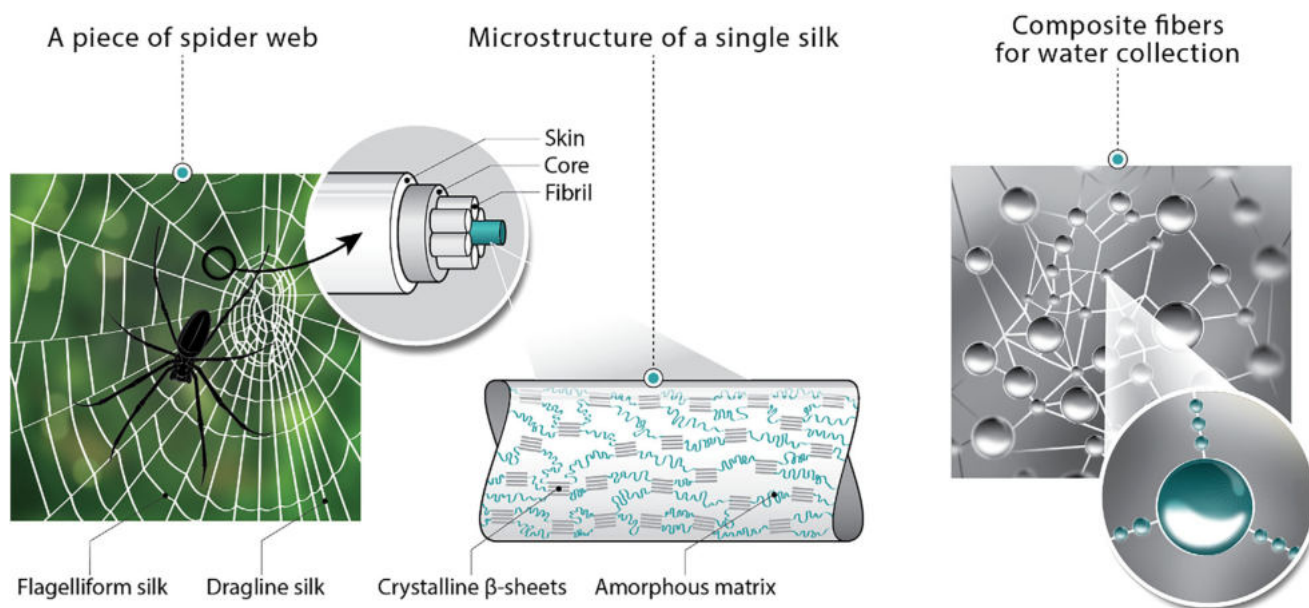


FIGURE 7 An illustration showing the spider silk structure and the silk-inspired composite fibers. Left, a schematic diagram of a typical orb web, a dragline silk and its core-shell structure; middle, a magnified structure of a spider silk composed of crystalline β -sheets in an amorphous matrix; right, an illustration of water collection through spider silk-inspired recombinant silk.

TABLE 3 Mechanical properties of five types of spider silk, Kevlar, and high-tensile steel.

Material	Tensile strength (GPa)	Extensibility (%)	Toughness (energy to failure) (MJ m^{-3})
Dragline ^{82,87,88}	0.9–1.5	21–27	136–194
Flagelliform silk ^{82,87,88}	0.5–1.3	119–270	75–283
Kevlar 49 ⁸²	3.6	2.7	50
High-tensile steel ⁸²	1.5	0.8	6
Carbon fiber ⁹	0.7	1.4	1.1

of MaSp2, provides the extensibility through the adoption of a 3_1 -helical conformation, enabling an efficient energy dissipation to prevent brittle failure. Meanwhile, the crystalline β -sheets, upon stretching, reinforce the partially extended and oriented protein chains by forming interlocking regions that contribute to the strength of the spider silk.^{80,82,83}

On the mesoscopic level (micrometer scale), fibrils oriented along the fiber axis to form the core of the fiber, resembling the structure of a rope. At the macroscopic level, the silk fiber exhibits a core-shell structure with fibril bundles forming the core,⁸¹ as shown in Figure 7. Ultimately, the unique combination of molecular structure, hierarchical organization, and efficient energy dissipation mechanisms creates a viscoelastic material with remark-

able strength, extensibility, and toughness, as summarized in Table 3.

3 | NATURE-INSPIRED HIERARCHICAL MATERIALS

As mentioned in Section 2, natural organisms exhibit a combination of unique hierarchical structures, exceptional mechanical properties, and remarkable adaptability to their surrounding environments. Astonishingly, they construct their precise, complex structures at ambient temperature and pressure using brittle or weak materials, such as HA, aragonite, or nanocrystalline proteins. Therefore, the outstanding performance of hierarchical natural materials, such as bone, nacre, sea sponge, and spider silk, is derived from their unique structures rather than from material selection. Naturally, engineers look to nature's examples of structural optimization for inspiration when designing the next generation of technology, especially when material selection reaches its limitations.

Since the term “biomimetics” was coined by Otto Schmitt in the 1950s,⁸⁹ and then introduced by Arthur Heuer into the ceramic community in 1990s,⁴ the field of nature-inspired or bioinspired material design has grown rapidly. This growth has been fueled by advances in materials science, nanotechnology, additive manufacturing, and, most recently, AI. Consequently, novel materials inspired by natural organisms are finding increasing

applications in diverse areas, including healthcare, energy, and sustainability.

3.1 | Healthcare

Tissue and organ failures resulting from trauma, disease, or aging have been reported to account for half of the annual healthcare expenditures in the United States.⁹⁰ Among them, bone is the second most commonly transplanted tissue, with blood being the first.^{91,92} For bone regeneration, autografts are the gold standard for treatment of bone defects, although they are limited by supply and donor site morbidity.⁹³ Allografts, obtained from living donors or cadavers of the same species, are alternatives to autografts, but they are expensive and suffer from potential risks such as disease transmission and adverse host immune response.⁹³ Inspired by the structure and properties of human bone, significant progress has been made over the past decades in designing synthetic materials that mimic the chemistry, structure, and functionality of natural bone tissue for bone regeneration. As discussed in Section 2.1, bone is a composite material, composed of collagen fibrils and HA. Consequently, both organic and inorganic biomaterials have drawn increasing attention for bone repair applications.

Biodegradable polymeric materials,^{94–97} calcium phosphate-based bioceramics such as HA, β -tricalcium phosphate (β -TCP), and biphasic calcium phosphate, a mixture of HA and β -TCP, all composed of the same ions as bone,^{18,22,67,98–100} as well as bioactive glass and glass-ceramics,^{67,101–111} have all been investigated for their potential in bone repair. These biomaterials serve as essential building blocks for creating matrices or scaffolds used in tissue engineering.

As an interdisciplinary field, tissue engineering applies the principles of biology and engineering toward the development of biological substitutes to restore, maintain, or improve tissue function.^{112,113} As illustrated in Figure 8, the most common tissue engineering approach involves using biomaterial scaffolds with well-defined structures. These scaffolds serve as temporary frameworks for cells, guiding their proliferation and differentiation into the desired tissue or organ. Growth factors and other biomolecules can be incorporated into the scaffolds along with the cells to regulate cellular functions during tissue or organ regeneration.^{112,113}

Particularly for bone tissue engineering, scaffolds must meet a stringent set of requirements to provide the necessary functionality. These requirements include supporting cell and tissue infiltration, facilitating the transport of nutrients, and being mechanically strong and tough

enough to bear the loads from normal activities, similar to how a host bone performs.^{20,23}

Inspired by the remarkable properties of natural materials such as bone and nacre, researchers are making significant efforts to mimic the architecture and function of these materials in designing new synthetic structures with similar or even superior performance. Although inorganic materials like calcium phosphate-based bioceramics and bioactive glass are inherently brittle, they possess appealing characteristics for bone tissue engineering, such as high mechanical strength under compression, excellent biocompatibility, and osteo-stimulatory ability through the release of ions.^{20,22,23,114}

Considerable progress has been made in creating porous scaffolds that mimic the structure of trabecular bone at the macroscopic scale using a variety of techniques. These methods include sol-gel methods, thermal bonding of particles, fibers, or spheres, polymer foam replication, foaming of suspensions, and 3D printing.^{20,22,23} For instance, 3D printing, a layer-by-layer assembly technique directed by computer-aided design, allows for the production of porous glass and ceramic scaffolds with precisely controlled architecture at the micrometer scale, as shown in Figure 4. These 3D-printed scaffolds with periodic structures have been reported to achieve compressive strength comparable to that of cortical bone while maintaining sufficient porosity to facilitate bone ingrowth.^{21,115,116} Using bone-like virtual templates for the printing of HA and bioactive glass trabecular scaffolds has been proposed,^{17,117–119} as well as some selected triply periodic minimal surfaces (TPMSs) that exhibit highly appealing similarities with trabecular bone architecture, such as zero-mean curvature and fully interconnected pores.^{120,121}

Additionally, attempts to mimic the “brick-and-mortar” structure of nacre using a freeze-casting technique have resulted in porous glass and HA with lamellar, oriented porosity and high compressive strength,^{19,122–125} as illustrated in Figure 5. Further details about bioinspired approaches to produce porous bioceramics and composites can be found elsewhere.¹²⁶ Despite their high compressive strength, these ceramic- and glass-based scaffolds suffer from low fracture toughness and low flexural strength due to the intrinsic brittleness of their constituent materials.^{20,22}

Inspired by the toughening mechanisms found in biological materials, various approaches have been explored to enhance the toughness of scaffold materials and to develop organic/inorganic composites through surface coating or infiltration or the use of composite materials or tough glass-ceramics.^{1,108,127} However, significant improvements in fracture toughness have yet to be validated. One primary challenge is that, unlike the

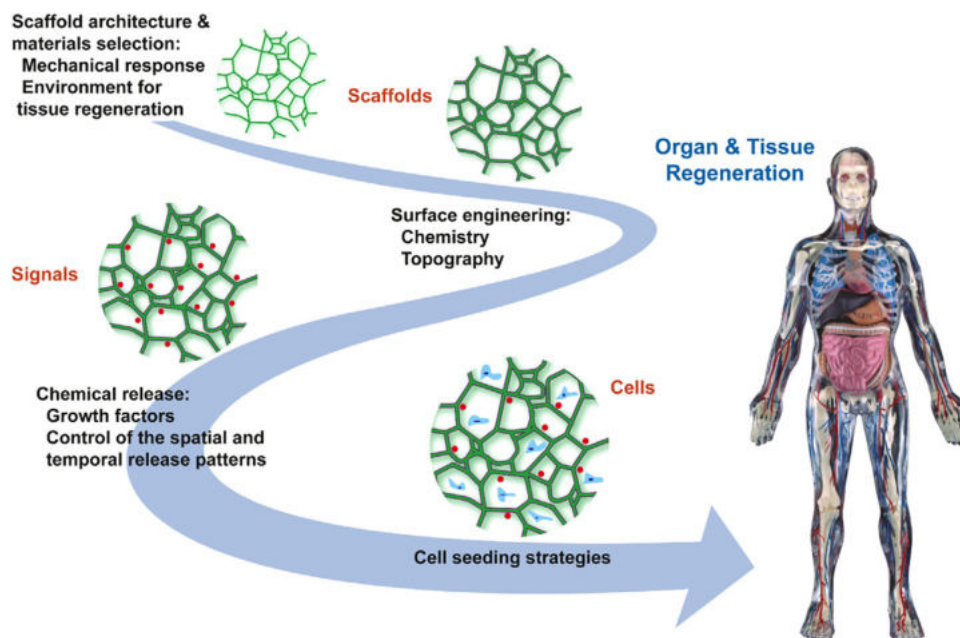


FIGURE 8 Three key components in tissue engineering: scaffolds, cells, and signals. *Source:* Image courtesy of Dr. Antoni P. Tomsia at the Lawrence Berkeley National Laboratory.

hierarchical composite structures of bone or nacre, the molecular and nano-level assembly of organic and ceramic constituents and the manipulation of their architecture across multiple length scales have not yet been fully achieved in these porous glass and ceramic-based scaffolds.^{20,128}

Owing to its remarkable extensibility, toughness, and biological properties, spider silk and its proteins, both natural and recombinant, have witnessed increasing interest in biomedical applications. Spider silks have been used in tissue engineering to support skin regeneration,^{31,129} bone and cartilage repair,^{130,131} nerve regeneration,^{27,30} vascularization,^{29,31,132} and drug delivery.^{28,133–135} Inspired by the hierarchical structure in biological materials, hybrid fibers consisting of oriented nano HA have been successfully nucleated on the surface of spider dragline through a controlled biomineralization process.¹³⁶ This approach represents a step toward fabricating hybrid scaffolds from bone and spider silk for tissue engineering. Further investigations on the apatite-coated spider silk have demonstrated the formation of a controlled and homogeneous coating composed of nanocrystals, which maintained the superior mechanical performance of silk, making it suitable to develop high-performance hybrid interfaces for bone tissue engineering.¹³⁷ Moreover, advances in the engineering of recombinant spider silk proteins have enabled the formation of calcium phosphates and the controlled collagen binding, an indication of their potential applications as biomaterials at the interface between tendon and bone.¹³⁸ Continued process optimization combined with

advanced manufacturing could potentially create porous bone scaffolds with hierarchical structures at both the nano- and microscale, enhancing strength and toughness.

Additionally, the mechanical properties of spider silk align well with the requirements of soft, elastic tissues such as skin, nerves, and blood vessels.^{27,29,30,129,132} Spider silk conduits have been found to support nerve regeneration by promoting the growth of neuronal cells.^{27,30} Furthermore, the unique architecture of spider silk allows for the incorporation of drugs or growth factors into its structure, enabling controlled release over time for localized delivery of therapeutic agents for cancer treatment.¹³⁵ The unique properties of spider silk-based materials clearly offer advantages in biomedical applications. However, the limited supply of natural spider silk and the difficulties in manufacturing recombinant silk with mechanical properties similar to its natural counterpart have posed significant challenges in materials science for decades.¹³⁹

In summary, inspired by natural materials like bone and nacre, significant advancements have been made in creating synthetic structures with comparable or superior performance to their counterparts. Additionally, spider silk, with its remarkable properties, presents a promising avenue for biomedical applications, including tissue engineering and drug delivery. However, achieving the molecular and nano-level assembly of organic and ceramic constituents to replicate the hierarchical structure of natural materials remains a complex task. Moreover, the limited supply of natural spider silk and the difficulties in producing recombinant spider silk with mechanical

properties equivalent to its natural counterpart present significant manufacturing challenges. Continued research, process optimization, and the development of advanced manufacturing techniques are essential to overcome these challenges.

3.2 | Energy

The rapidly growing demand for portable mobile devices and electric vehicles has spurred intense research efforts into high-performance electrochemical energy storage (EES) devices. These devices need to store a large amount of energy (high energy density) while being able to charge and discharge rapidly (high power density).^{140–148} Among the four primary types of EES devices—capacitors, supercapacitors, batteries, and fuel cells—batteries have emerged as the preferred option due to their ideal combination of high energy densities (≥ 100 Wh kg⁻¹), long lifecycles, and fast charging rates,^{149,150} which meet the rigorous requirements of modern applications.

Since the groundwork was laid by Stanley Whittingham, John Goodenough, and Akira Yoshino in the 1970s and 1980s,^{151–158} lithium-ion batteries (LIBs) have revolutionized not only consumer electronics but also the broader landscape of energy storage and consumption.^{140–148} Their widespread adoption has been driven by their ability to provide reliable and efficient power to a wide range of devices, from smartphones and laptops to electric vehicles and grid storage systems. This transformative technology has been catalyzing continuous advancements in battery technology, focusing on enhancing performance, safety, and cost-effectiveness to keep pace with the increasing energy demands of contemporary society.^{140–148}

As depicted in Figure 9A, an LIB is composed of an anode, a cathode, a liquid electrolyte facilitating lithium ion migration between these electrodes, and a porous separator to prevent short circuits.^{149,159} In LIBs, lithium ions undergo transportation and intercalation between the two insertion host electrodes, where redox reactions transpire within their active materials during the charge–discharge cycles. The performance of these batteries is highly dependent on the active electrode materials utilized in their construction, whereas the other components are passive but indispensable in facilitating functionality.

Graphite, an intercalation/insertion material, has dominated the anode market since its commercialization by Sony in 1991,¹⁴⁸ attributed to its high practical specific capacity (~ 360 mA h g⁻¹ vs. theoretical 372 mA h g⁻¹), low operating potential (~ 0.2 V vs. Li⁺/Li), and stable discharge profile.^{160–164} Lithium titanate (Li₄Ti₅O₁₂) spinel oxide, introduced in the 2000s, offers high power density, extended cycle life, and superior safety, although it pos-

esses a lower energy density (175 mA h g⁻¹) compared to graphite.^{164,165} Silicon-based anode materials, boasting high energy density (3572 mA h g⁻¹) and volumetric capacity (8322 vs. 841 mA h cm⁻³ for graphite), present a promising alternative with capacities up to 10 times greater than graphite.¹⁶⁶ However, their substantial expansion during charging (320%) results in capacity loss and fading, an issue that remains to be addressed.^{166,167} Other potential materials under investigation include lithium (Li), tin (Sn), tin oxide (SnO₂), carbon nanotubes (CNTs), and graphene, all of which offer high capacity but encounter challenges related to mechanical stability and cyclability.^{167–171}

The cathode plays a critical role in determining a battery's capacity, voltage, and overall performance. Commonly used cathode materials are made out of lithium metal oxide, including layered LiMO₂ (M = Mn, Co, and Ni),¹⁵² olivine LiFePO₄ (LFP),¹⁷² and spinel LiMn₂O₄ (LMO).¹⁷³ Among these, the layered LiCoO₂ cathode, first identified as an intercalation cathode material in 1980,¹⁵² offers high lithium-ion conductivity, stable discharge current, and long cycle life. These properties have made it the dominant cathode material in the portable electronics market for over 40 years.^{168,174} However, the high cost, toxicity, and chemical instability at deep discharge associated with LiCoO₂ limit its uses for electric vehicles and stationary storage applications.^{164,168,175} Conversely, LFP batteries are gaining increased adoption in low-end vehicles due to their cost advantages, enhanced safety, longer lifecycles (>2000 cycles), and less environmental impact.^{176–178}

Over the last two decades, significant research efforts have concentrated on developing high-performance cathode materials for next-generation LIBs to meet the demanding standards of electric vehicles and large-scale energy storage. Nickel-based layered oxides, Li[Ni_aCo_bMn_c]O₂ ($a + b + c = 1$; NCM) and Li[Ni_{1-x-y}Co_xAl_y]O₂ (NCA) offer high energy density, up to 300 Wh kg⁻¹, making them a popular choice for high-end electric vehicles.^{164,179} However, the limited availability of key components such as cobalt and nickel, along with environmental concerns, continues to pose significant challenges for the widespread adoption of these batteries.¹⁷⁶ Numerous research activities in both academia and industry are focused on further improving energy densities to approximately 350 Wh kg⁻¹ at the cell level, aiming to enhance driving performance and reduce costs.¹⁷⁹

The overall performance of batteries, particularly at the cell level, is profoundly influenced by both the selection of materials and their structural configuration. Achieving an optimal balance between ion transport, electron conductivity, and mechanical stability during operation represents a multifaceted engineering challenge.^{169,180–182} In nature, the leverage of porous architectures to facilitate fluid

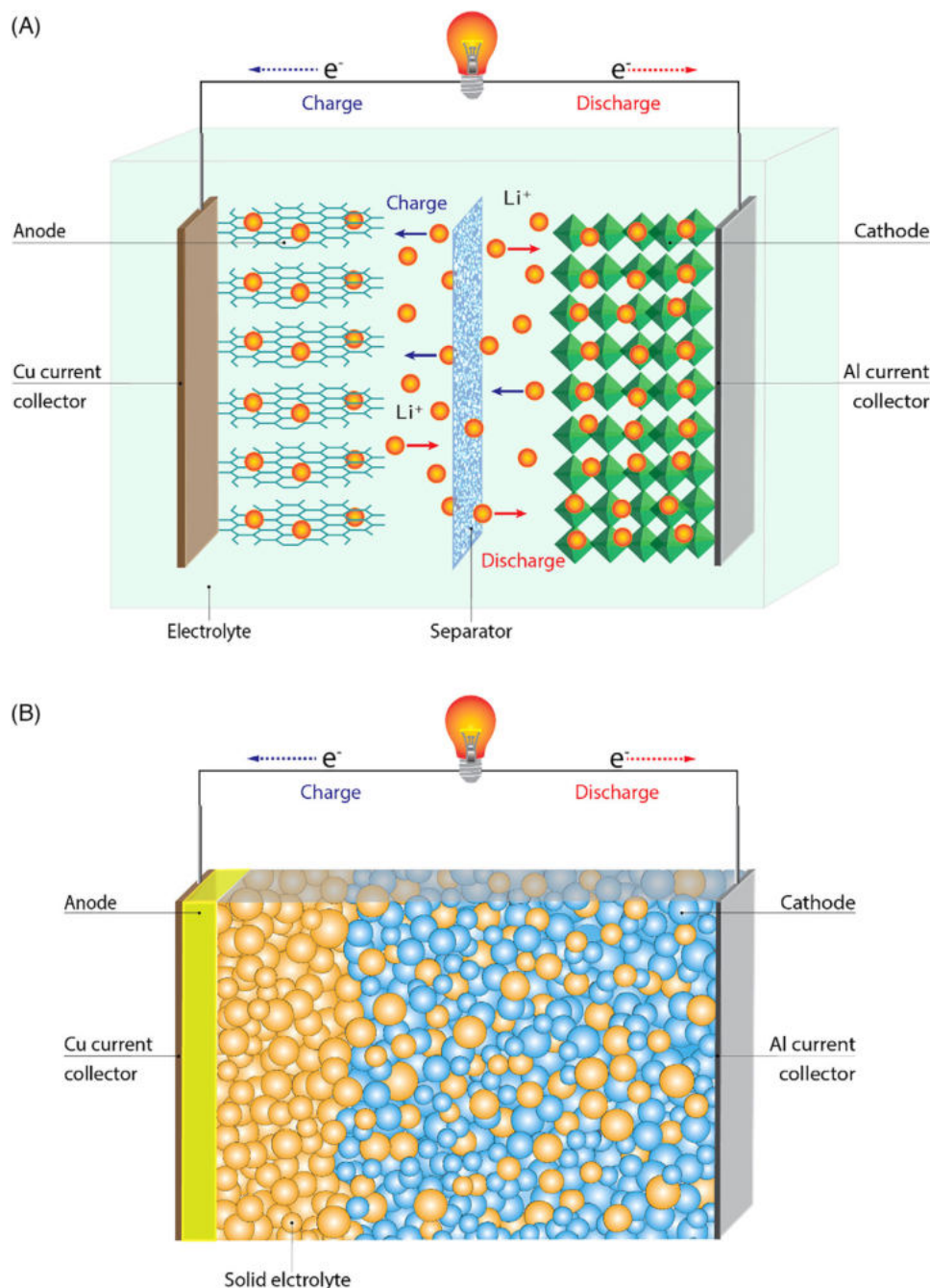


FIGURE 9 A schematic illustration of (A) a conventional rechargeable lithium-ion battery (LIB) consisting of an anode and a cathode sandwiched between two current collectors and isolated by a porous separator in a liquid electrolyte and (B) an all-solid-state battery (ASSB) consisting of a metal anode, a cathode, and a solid electrolyte.

irrigation across multiple length scales, as exemplified by bone (Figure 4), and the implementation of hierarchical structures to attain high tensile strength, as demonstrated by spider silk (Figure 7), are prevalent strategies that contribute to their functional efficacy.

Inspired by the hierarchical structure of natural materials such as bone, there has been a growing interest in the fabrication of 3D porous architectures as conductive scaffolds for various electrode materials to improve battery

performance at cell level.^{182,183} A typical 2D electrode with a planar current collector can provide sufficient charge to meet the requirements of the electrode materials but at a limited depth. In contrast, a 3D electrode architecture, composed of a 3D porous conductive scaffold for electron transport and a fully interconnected hierarchical architecture for ion transport, can significantly enhance efficient ion transport.^{180–182} For example, a 3D porous holey graphene framework/ Nb_2O_5 composite electrode

fabricated using a self-assembly technique demonstrates a capacity retention much higher than graphite, silicon, or carbon–silicon anodes at high mass loading and high current density as a result of efficient electron and ion transport pathways.^{180,181}

Using a 3D printing technique, LIBs with precise design and hierarchical architecture have been fabricated using a variety of inks, including LTO and LFP,^{184,185} cellulose nanofiber–infiltrated Li metal and LFP,¹⁸⁶ graphene oxide–based LTO and LFP,¹⁸⁷ CNT-based LTO and LFP,¹⁸⁸ and holey graphene oxide.¹⁸⁹ By creating a 3D porous scaffold composed of interconnected porosity, these batteries have demonstrated high areal capacity in customized form factors,^{185,188} which can be potentially integrated into wearable electronics or other related applications.

Inspired by the “brick-and-mortar” structure in nacre (Figure 5), porous $\text{LiNi}_{0.8}\text{Co}_{0.15}\text{Al}_{0.05}\text{O}_2$ (NCA) cathodes, prepared using a freeze-casting method with controlled, aligned porosity, enabled a three- to four-fold increase in areal capacity compared to typical composite electrode.¹⁹⁰ A similar finding is also reported in a freeze-cast $\text{LiNi}_{0.8}\text{Co}_{0.1}\text{Mn}_{0.1}\text{O}_2$ (NCM) cathode, which led to a high areal energy density (15.1 mWh cm^{-2}) at high mass loading (26 mg cm^{-2}) due to its hierarchical porous architecture.¹⁸³ Last but not least, the unique hierarchical structure and the high toughness of spider silk (Figure 7) have inspired the exploration of using it as a binder in electrodes to reduce the volumetric cyclical change associated with silicon anode materials,¹⁹¹ or the development of novel binders such as (poly(acrylic acid)-supramolecular poly(urethane-urea)) to generate a strong adhesion between electrodes (LCO cathode and graphite anode) and current collectors, which is of great significance for flexible LIBs with high energy density.¹⁹²

As an alternative approach to achieve higher energy density, longer cycle life, and improved safety, all-solid-state batteries (ASSBs) have received considerable attention in both academia and industry.^{169,193–201} As illustrated in Figure 9B, an ASSB is composed of a metal anode, a solid electrolyte, and a high-voltage cathode. These components are engineered to work with solid materials for the desired performance characteristics. The replacement of the flammable liquid electrolyte in traditional LIBs with solid electrolyte in ASSBs substantially improves safety and contributes to potentially longer device lifetimes, exceeding 1000 cycles.^{169,202,203} Furthermore, the use of solid electrolyte enables the integration of high-performance metal anodes, such as lithium (Li), sodium (Na), silicon (Si), and magnesium (Mg), to achieve the highest capacities and operating voltages.^{204–206}

High ionic conductivity is a key characteristic of solid electrolytes. Additionally, for practical applications in EES and conversion systems, solid electrolytes must satisfy

several other stringent requirements,^{200,207–211} including low ionic area-specific resistance, high electronic area-specific resistance, excellent ionic selectivity, a broad electrochemical stability window, chemical compatibility with other components, superior thermal and mechanical stability, scalable and straightforward fabrication processes, cost-effectiveness, ease of device integration, and environmental sustainability.

Over the past two decades, numerous solid electrolytes with promising ionic conductivities have been developed,²⁰⁰ including NASICON-type $\text{Li}_{1.5}\text{Al}_{0.5}\text{Ge}_{1.5}(\text{PO}_4)_3$ (LAGP),²¹² $\text{Li}_{1.3}\text{Al}_{0.3}\text{Ti}_{1.7}(\text{PO}_4)_3$ (LATP),^{213,214} garnet $\text{Li}_7\text{La}_3\text{Zr}_2\text{O}_{12}$ (LLZO),^{215,216} sulfides, such as $\text{Li}_{10}\text{GeP}_2\text{S}_{12}$ (LGPS),²⁰¹ and $\text{Li}_7\text{P}_3\text{S}_{11}$ (LPS),^{193,217} thin films based on LiPON,^{218,219} and polymer electrolytes (e.g., poly(ethylene oxide) [PEO]).^{220,221} Inorganic electrolytes, in particular, possess a high mechanical modulus, which aids in suppressing lithium dendrite growth.^{222,223} However, the ceramic electrolytes exhibit low fracture toughness, rendering them susceptible to external mechanical impacts and posing considerable challenges for scalable cell fabrication.

One potential solution to these mechanical limitations is inspired by nacre for the design of layered solid electrolytes that combine ceramic materials, such as LAGP, with polymer electrolytes such as PEO, poly(ether-acrylate), and epoxy. The composite electrolyte demonstrates a much higher fracture strain (1.1%) than pure ceramic LAGP electrolytes (0.13%) and a much larger ultimate flexural modulus (7.8 GPa) than polymer electrolytes (20 MPa). These hybrid architectures help suppress dendrite growth while accommodating mechanical stress during cycling, offering a promising pathway for overcoming the mechanical challenges associated with solid electrolytes.²²⁴ In another example, using a freeze-casting method, a porous LLZO scaffold with a lamellar structure, similar to those in nacre, was fabricated to make an ASSB with a porous/dense/porous tri-layer.²²⁵ The porous scaffolds were infiltrated with $\text{LiNi}_{0.6}\text{Mn}_{0.2}\text{Co}_{0.2}\text{O}$ active materials on one side and metallic Li on the other to enable excellent discharge capacity of $125\text{--}135 \text{ mA h g}^{-1}$.²²⁵

As can be concluded from the discussion above, the continuous evolution of electrolyte, cathode, and anode materials, coupled with innovative structural configurations, is essential in advancing LIB and ASSB technologies. Concurrently, adopting nature-inspired hierarchical structures and integrating nanomaterials within 3D electrodes and electrolytes addresses critical challenges in ion transport, electron conductivity, and mechanical stability. These advancements, supported by cutting-edge manufacturing techniques like 3D printing and freeze casting, are paving the way for next-generation batteries that promise

enhanced energy densities, longer lifespans, and superior safety.

3.3 | Sustainability

The exponential increase in population and industrialization has led to the accelerated consumption of nonrenewable petrochemical resources, significant global pollution, and climate change.²²⁶ It is imperative to identify novel strategies for fostering a more sustainable ecosystem, where materials play a crucial role in shaping the sustainability landscape due to their lifecycle impacts on the environment, economic development, and the well-being of the global population. Sustainable development, often defined as “development that meets the needs of the present without compromising the ability of future generations to meet their own needs,”²²⁷ necessitates prudent management of natural renewable resources and the advancement of technologies to optimize the use of finite materials, as illustrated by the circular economy model in Figure 10—the “sustainable butterfly diagram” by the Ellen MacArthur Foundation.²²⁸

This diagram delineates two primary cycles: the biological cycle, which includes processes involving renewable resources and emphasizes the sustainable management of biological materials and nutrients; and the technical cycle, which involves finite materials and products that must be maintained in a closed loop to minimize waste and resource extraction through practices such as reuse, repair, remanufacture, and recycling.²²⁹ The diagram provides a holistic approach to the circular economy and underscores the importance of nature-inspired designs for sustainable development.¹⁰

In the biological cycles, natural organisms are distinguished by their capacity to construct intricate hierarchical structures across multiple length scales, utilizing limited resources under ambient temperature and environmental pressure through evolution. These biological materials exhibit multifunctionality and self-healing properties, enabling adaptation to changing environments.^{8,11} Consequently, insights derived from the biological cycles have consistently provided inspiration for fostering sustainable development within the technological cycles.^{10,229,230}

Examples include the application of natural wood in advanced civil engineering to achieve carbon-negative buildings and advanced functionality^{230,231}; the creation of sustainable fiber technologies inspired by the structural and mechanical property of spider silk²³²; the use of biological molecules (e.g., enzymes, proteins, or microorganisms) as bioelectrocatalysis system for biosensing, renewable bioelectricity, and the synthesis of valuable chemicals^{233–236}; the development of modular bioinor-

ganic hybrids consisting of efficient light-harvesting nanoparticles and microorganisms to enable biomanufacturing processes^{237,238}; the production of engineered living materials capable of self-organization and self-repair^{239–241}; and the use of biomineralization process such as microbial-induced carbonate precipitation (MICP) or dissolved inorganic carbon to sequester CO₂.^{242–246}

Inspired by the efficient pathway for carbon sequestration and conversion in the biological ecosystems, such as forests and aquatic systems, significant efforts have been devoted to optimizing the MICP process for improved efficiency and environmental sustainability.^{242,243,245,247,248} As illustrated in Figure 11, MICP occurs when bacteria secrete urease to hydrolyze urea into CO₂ and NH₃. The alkaline environment from NH₃ converts CO₂ into CO₃²⁻, whereas bacteria absorb Ca²⁺ onto their negatively charged surfaces. The interaction of Ca²⁺ and CO₃²⁻ forms calcium carbonate crystals, which deposit on bacteria, binding particles into solid structures for carbon sequestration.^{242,249,250} One limitation of the approach is that the ureolytic MICP requires a constant supply of urea and generates a large amount of ammonia as a byproduct, making it challenging for long-term CO₂ sequestration.^{251–253} A recent approach by combining MICP and photosynthesis offers a fresh perspective on the process.²⁴³ In this study, photosynthetic living materials designed for dual CO₂ sequestration are developed by embedding the MICP-capable photosynthetic cyanobacterium *Synechococcus* sp. strain PCC 7002 within a 3D-printed Pluronic F-127 (F127)-based polymeric matrix. The resulting bio-printed structures enable dual-carbon capture through biomass production and the formation of insoluble carbonates, continuing to sequester carbon throughout their lifecycle for over 1 year.²⁴³ This suggests the high potential of photosynthetic living materials for efficient, scalable carbon capture, supporting carbon-neutral infrastructure and CO₂ mitigation.

In parallel, concrete ranks as the most extensively utilized engineering material globally, surpassed only by water in terms of overall consumption.²²⁹ This widespread usage is attributed to its versatility, durability, and cost-effectiveness.²⁵⁴ By integrating principles derived from biological systems, advancements in concrete technology continue to evolve, aiming to enhance its sustainability, durability, and multifunctionality in line with the innovations observed in natural materials.^{229,254,255} One of the major challenges in concrete infrastructure is the occurrence of cracks, whether autogenous or caused by mechanical loading, as these can compromise the safety and durability of structures. Self-healing concretes have used both autogenous and autonomous approaches to achieve the repair of small cracks without human intervention.²⁵⁶

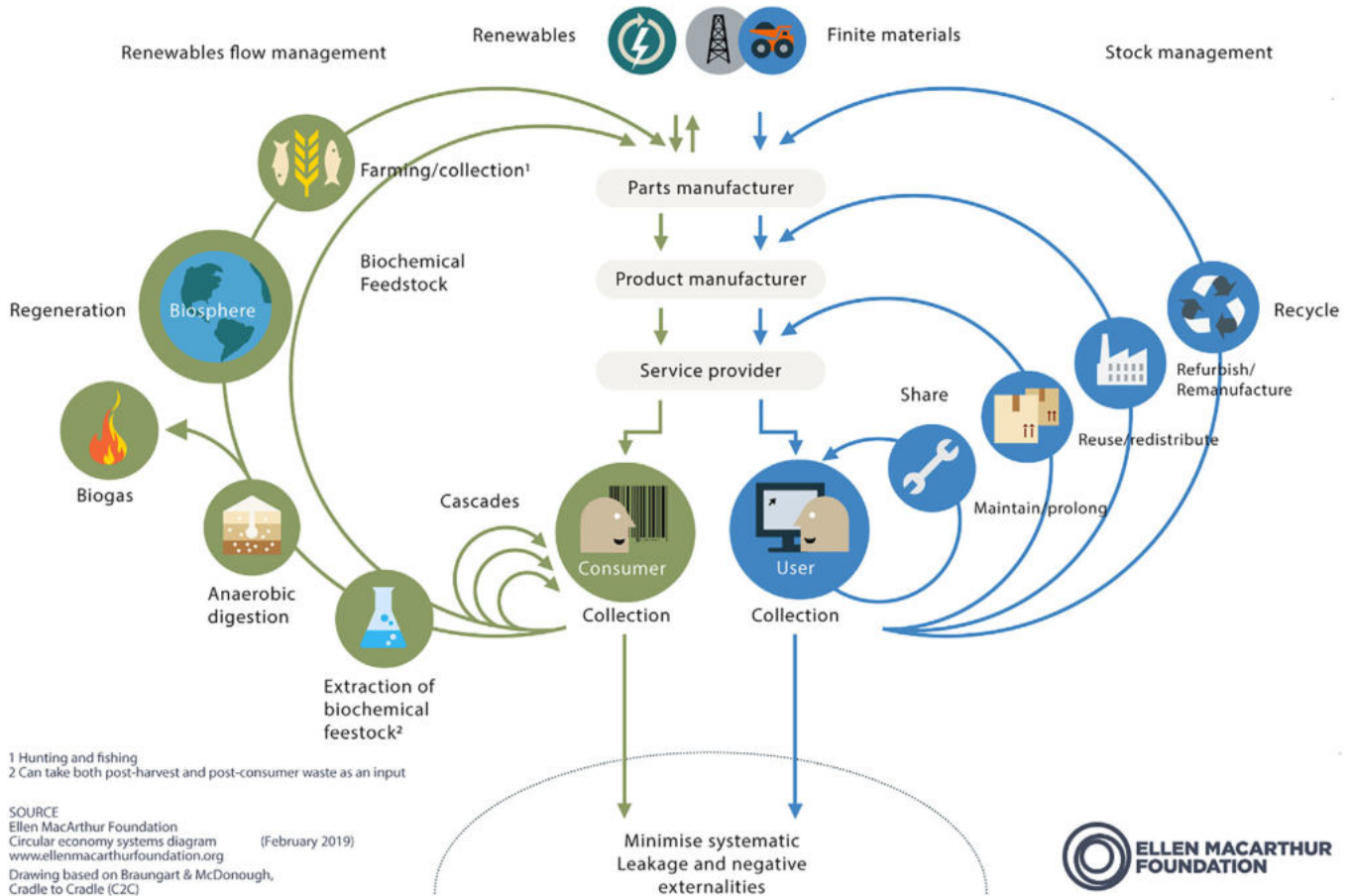


FIGURE 10 The butterfly diagram of the circular economy illustrates the continuous flow of materials in a sustainable system. It highlights two main cycles: the biological cycle, where biodegradable nutrients return to the ecosystem, and the technical cycle, where products and materials are kept in use through reuse, repair, remanufacture, and recycling.²²⁸ Source: Reproduced from Ellen MacArthur Foundation, 2025, www.ellenmacarthurfoundation.org, with permission.

As illustrated in Figure 12, the autogenous self-healing relies on intrinsic physical, chemical, and mechanical mechanisms, including (1) expansion of hydrated concrete matrix, (2) continued hydration, (3) carbonation of calcium hydroxide, and (4) crack blockage by fine particles from water or cracking shedding.^{257–259} Alternatively, autonomous self-healing utilizes advanced technologies, such as electrodeposition, shape memory alloys, encapsulated healing agents, vascular systems, and microbial methods.²⁵⁶ For example, polymeric capsules have demonstrated their ability to resist the concrete mixing process and to break when cracks appear, obtaining complete sealing of the crack with chemical agents.^{260,261}

Additionally, drawing on the principles of biomineralization in natural organisms, efforts have been made to develop self-healing concretes, which incorporate bacteria that can precipitate calcium carbonate.^{241,255–257,262} When cracks form and rainwater enters them, the dormant bacterial spores become active, consuming a nutrient source also embedded in the concrete. As a result of

the metabolic process, calcium carbonate is precipitated, which autonomously fills the spaces of the cracks and restores the concrete's structural integrity.^{263–266} Although most of these studies are conducted at lab scale under static loading and much research is needed to identify proper bacteria for prolonged periods, they have the potential to enhance the longevity of concrete structures for sustainable development of infrastructures.

Similarly, the collection of water from the atmosphere as a sustainable water source is of great significance, which is especially critical in arid areas where water scarcity poses a significant threat to the global population.²⁶⁷ Spider silk, in addition to its remarkable extensibility and toughness, also exhibits unique water-collecting abilities,^{268,269} as illustrated in Figure 7. Due to its unique wettability, resulting from a periodic spindle-knot structure, spider silk uses the cooperation of multi-gradients to drive tiny droplets toward the spindle-knots for efficient water collection.²⁶⁸ Based on this characteristic, numerous bioinspired fibers have been fabricated for water collection.^{270–272} In a recent

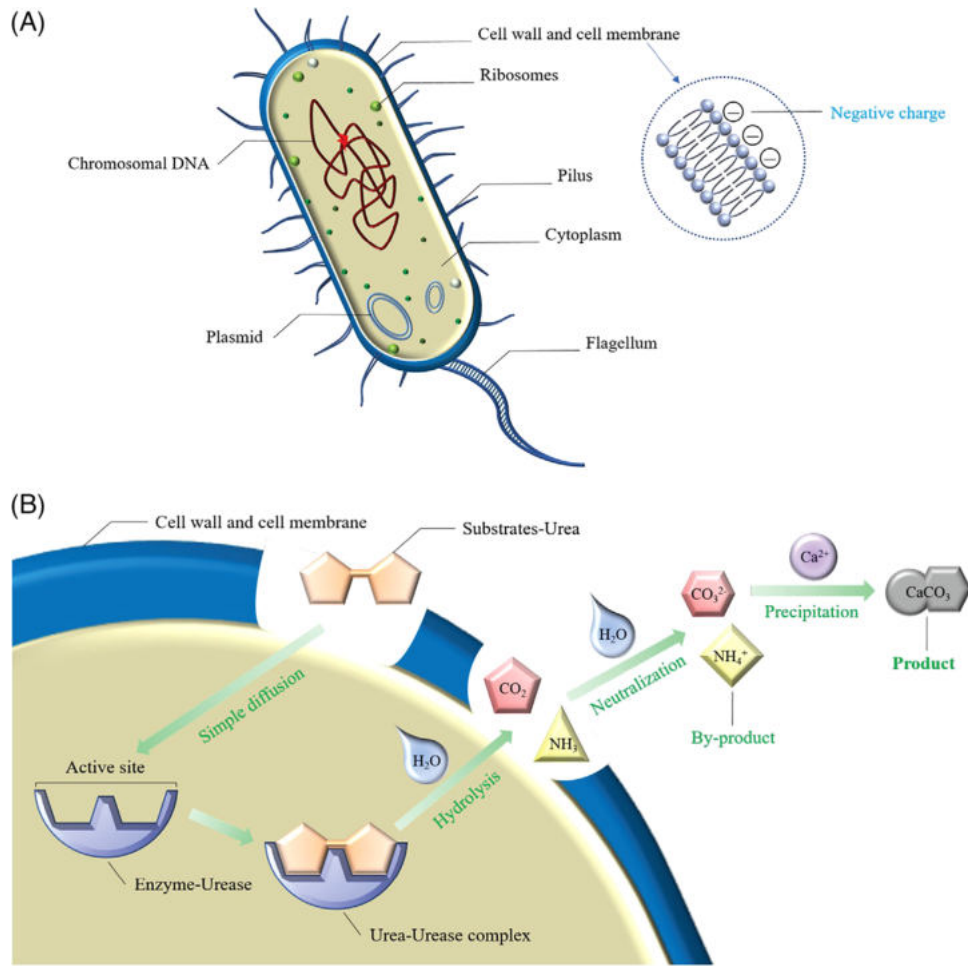


FIGURE 11 Schematic drawing for the microbial-induced carbonate precipitation (MICP) process: (A) cell membrane of *Sporosarcina pasteurii*; (B) principles of the MICP reaction. Source: Reprinted with permission from Ref. [242], Springer Nature.

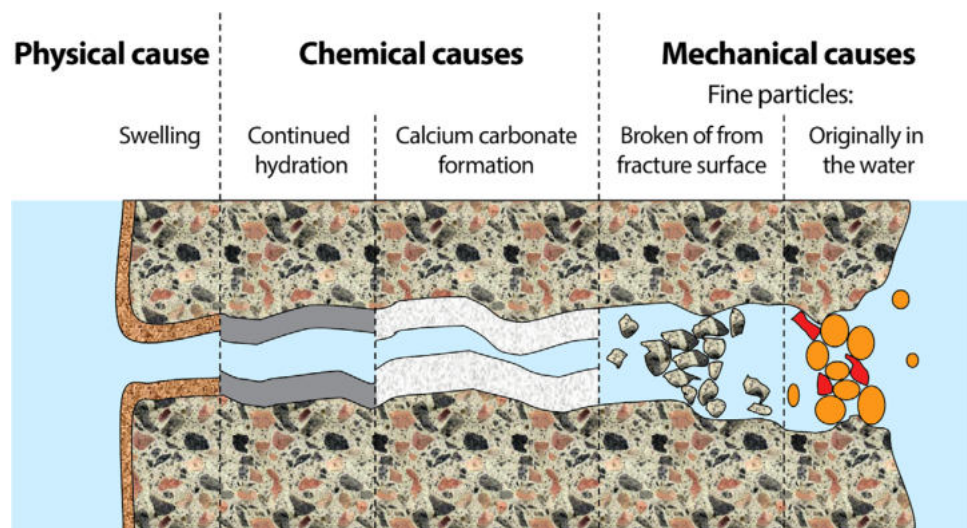


FIGURE 12 Different mechanisms of autogenic self-healing in concrete.²⁵⁷ Source: Reprinted with permission from Ref. [257], Springer.

study, the creation of an all silk-protein fiber with periodic knots enables extremely high volume-to-mass water collection capability, 100 times higher than the existing best water collection nonprotein artificial fibers, owing to the synergistic effect of the geometrical structure and hydrophilicity of silk protein materials.²⁷⁰ With the recent advances in the recombinant of artificial spider silk,¹³⁹ spider silk-inspired water collection systems hold the potential to make a significant impact on global water sustainability, demonstrating once again that nature's engineering can inspire groundbreaking solutions for modern challenges.

To sum up, nature's ability to create hierarchical structures with multifunctional properties using minimal resources provides valuable insights for sustainable development. Materials innovations inspired by natural organisms, such as MICP for carbon sequestration, self-healing concrete, and spider silk-inspired water collection systems, demonstrate the potential for nature-inspired materials to address pressing sustainability challenges.

4 | AI-ENABLED ORGANISM UNDERSTANDING AND MATERIAL DESIGN

AI refers to the capability of a machine, such as a robot, to autonomously replicate cognitive processes typically associated with human intellect. This includes making decisions based on its perception of the environment to achieve predefined objectives.²⁷³ Over the past two decades, AI has revolutionized and reshaped numerous sectors globally. The evolution of the machine learning (ML) method, a subset of AI, in the early 2010s has significantly expanded the scope and ambition of scientific discovery processes in multiple fields,^{274–281} including weather forecasting,²⁸² magnetic control of nuclear fusion reactors,²⁸³ hydropower station location planning,²⁸⁴ exploration of parameter space of particle accelerators,²⁸⁵ protein prediction and design,^{277–279} and cancer treatment.²⁸¹ ML encompasses a variety of methods, including (1) simple linear or logistic regressions; (2) tree-based methods such as decision trees and random forests; (3) artificial neural network-based methods such as feedforward neural networks or multilayer perceptrons, conventional neural networks, recurring neural networks, generative adversarial networks, variational autoencoders (VAEs), and graph neural networks; and (4) kernel-based methods such as Gaussian process regression and support-vector machine.^{274,276,280,286,287} These methods can be broadly categorized into three primary types: supervised learning, unsupervised learning, and reinforcement learn-

ing, each with distinct characteristics, applications, and methodologies.^{274–276}

AI has been increasingly employed for the prediction and engineering of proteins, which are fundamental components of natural organisms. To date, the structures of approximately 200 000 unique proteins have been determined experimentally and included in the Protein Data Bank (PDB).²⁸⁸ However, this number represents only a minuscule fraction of the billions of unknown protein sequences that exist.²⁸⁹ The breakthrough in de novo protein design through computational modeling and its validation through experimental synthesis by David Baker and his team demonstrated for the first time the possibility of creating entirely new proteins with specific structures and functions that do not exist in nature.²⁹⁰ The recent application of deep learning (DL), a subset of ML techniques using more complex neural network layers, facilitates the rapid and accurate prediction of 3D protein structures directly from their amino acid sequences. This capability not only provides critical insights into the functions of proteins with previously unknown structures but also aids in the design of novel proteins with advanced functionality.^{278,279,291,292} Using the DL-based model AlphaFold 2, Demis Hassabis and John Jumper further optimized the accuracy of protein structure prediction to about 1 Å.^{279,291} These advancements in protein structure prediction and engineering have significant implications for various fields, including biotechnology,^{293,294} medicine,^{281,295} and synthetic biology.²⁸⁰

Intrigued by recent advancements in the prediction and design of complex protein structures via DL and the concomitant increase in computational power, researchers have endeavored to elucidate the relationship between the primary sequences of various silk proteins in spider silk and their mechanical properties.^{296–301} Through a concerted effort, silk gene sequences from 1098 spider species were obtained, and the properties (mechanical, thermal, structural, and hydration) of dragline silks from 446 species were rigorously tested. The goal was to correlate gene sequences with mechanical performance and to establish a “sequence-material property” database.²⁹⁶ Their research indicates that silk gene sequence motifs, amino acid composition, and mechanical properties exhibit common features across diverse protein lineages. Their findings highlight the critical role of major ampullate spidroins (1–3 paralogs) and specific amino acid motifs in determining the measured properties of dragline silks from various spider species. Furthermore, their gene sequence database provides a foundational framework for future analyses of silk proteins and the de novo design of artificial spider silk.²⁹⁶ Utilizing this dataset and other existing silk protein data, a generative large-language model (LLM) based on DL methods has been developed to advance the

fundamental understanding of the relationship between spider silk sequences and their properties and to generate silk sequences with novel property combinations not found in natural silks.³⁰¹ This spidroin generative model has potential applications beyond spider silk, extending to other proteins with hierarchical structures for design objectives across multiple domains.

Concurrently, AI is increasingly being applied in materials science to enhance and accelerate the discovery of new materials. The AI tools allow for efficient hypothesis generation, optimized experimental design, large-scale data collection and interpretation, and the creation of actionable, reliable models that are seamlessly integrated into scientific workflows for streamlined discovery.^{274,287,303–309} ML algorithms, combined with existing materials data, are creating a materials intelligence ecosystem to support the development of surrogate models for predicting material properties and performance. As illustrated in Figure 13, materials intelligence ecosystems consist of four key interconnected components: (1) online repositories, (2) data representation, (3) modeling, and (4) validation.²⁸⁷

Computational modeling can be carried out at multiple length and time scales, from sub-nanometer (atomic) to meter scale (macro), and from femtosecond (fs) to second (s); thus, numerous methods are developed,³¹⁰ as categorized in Figure 14. One of the main challenges in choosing a modeling method is the conflicts between computing demand and the accuracy of results in a reasonable amount of time; that is, methods providing accurate results usually require more computational power and/or more time, whereas faster methods typically use more gross approximations. ML has been applied in each of these domains and can be used to integrate the methods to boost computational studies by improving simulation time and system size.³¹⁶ Using a large and diverse dataset composed of 607 683 stable inorganic structures, with up to 20 atoms in the unit cell,³¹⁷ from the Materials Project and Alexandria,^{318–320} researchers successfully trained MatterGen, a DL-based diffusion process generative model, for designing stable, novel, and diverse inorganic materials across periodic table.³⁰⁷ Structures generated by MatterGen are demonstrated to be more than twice as likely to be novel and stable and more than 10 times closer to the local energy minimum compared to previous models.^{307,320,321} The generative model, with its designation and promise to generate new objects, may serve as a foundation for the future inverse design of novel inorganic materials that are not currently known.

In the field of bioinspired materials design, the use of transformer-based deep generative models, a subset of DL models, shows promise in creating innovative designs that balance strength and toughness in nacre-inspired structures by correlating microstructure with their mechan-

ical properties.³²³ Additional AI algorithms, including Bayesian optimization and multimodal learning, are being explored to unlock the possibilities in the design and optimization of bioinspired ceramics.^{306,324} Although AI has made tremendous progress in advancing the field of bioinspired and biological materials by enabling the analysis, prediction, and design of complex systems, its application also faces several unique challenges due to the complexity, variability, and multiscale nature of biological materials.

For example, natural biological composites are renowned for their exceptional mechanical performance, which is attributed to their hierarchical structures spanning multiple length scales. These materials, like nacre shown in Figure 15, are constructed through the integration of organic proteins and inorganic crystalline phases into intricate architectures in a bottom-up manner. Recent advances in ML have enabled the prediction of complex protein structures,²⁷⁹ and the design and 3D printing of innovative bioinspired architectures,³²² demonstrating the potential of AI in this field. The modeling and synthesis of a spider web-inspired 3D structure is achieved by using a combination of three DL models, that is, an analog diffusion model, a discrete diffusion model, and an autoregressive transformer architecture, which allows for “learning” of the key geometric parameters in spider webs and constructing graphs for different design purposes. In addition, these DL-designed structures were then 3D-printed for mechanical evaluation to generate experimental data for further optimization of the structural designs.³²² In another example, a nacre-inspired cement–resin composite with superior mechanical robustness than its counterpart is demonstrated through the optimization of its gradient structure using an ML-assisted method.³²⁵ An integrated data-driven ML method based on a backpropagation neural network and a genetic algorithm allows for the forward prediction and reverse design of the “brick-and-mortar” structure in nacre by using cement and resin. The fabricated gradient composite shows an extraordinary combination of high flexural strength, toughness, and impact resistance, far exceeding the homogenous or heterogenous structures made from the same materials.³²⁵ Additionally, ML approaches were used to design and select TPMS architectures with optimized biomechanical features for bone tissue engineering applications³²⁶; then, the most promising structures from diamond, gyroid, and IWP classes were eventually printed by vat photopolymerization to fabricate HA scaffolds.³²⁷

It is clear that recent advancements in ML have demonstrated its potential for analyzing hierarchical biological materials across multiple length scales and designing novel composites and architected materials.^{328–333} One of the key challenges in these approaches is finding effective methods to describe complex hierarchical structures in

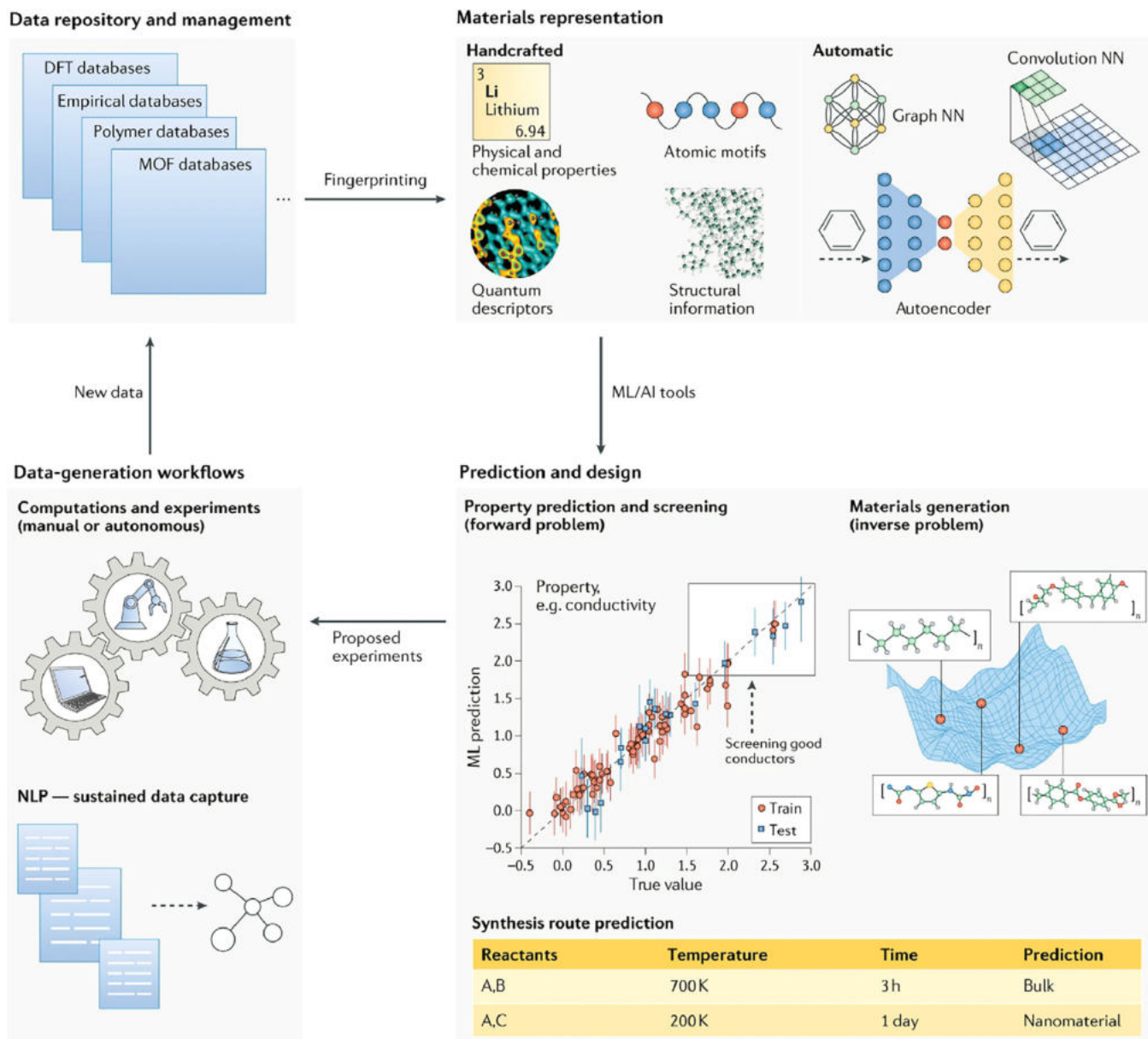


FIGURE 13 Material intelligence ecosystems comprise four interconnected components: (1) online repositories; (2) data representation; (3) modeling; (4) validation. DFT, density functional theory; MOF, metal–organic framework; NN, neural network. *Source:* Reprinted with permission from Ref. [287], Springer Nature. The image for property prediction and screening is reprinted with permission from Ref.[302], Elsevier. The graph for the graph neural network is reprinted with permission from Ref. [303], APS.

a simplified, reduced-dimensional framework. Such an approach, similar to coarse-graining techniques, allows for the physical relationships within these structures to be more efficiently learned, modeled, and utilized to address inverse design problems.³²⁸ By integrating a discrete autoencoder model, specifically the vector quantized VAE (VQ-VAE),²⁹¹ with an attention-based diffusion model,^{330,334} as depicted in Figure 16, a robust approach has been established for “learning” complex hierarchical microstructures and “speaking” the design language for both forward and inverse design of novel materials.^{328,335}

This integrated framework has been validated through the fabrication and testing of 3D-printed metallic honeycombs composed of copper and nickel, which were engineered to meet specific nonlinear stress–strain responses.^{328,335} Notably, the encoding generated by the VQ-VAE model operates independently of the downstream diffusion model, making it a versatile tool for a wide range of material properties beyond mechanical responses.

Even more recently, LLMs—generative AI models trained on vast corpora of text, typically comprising general information from articles and websites—have emerged as

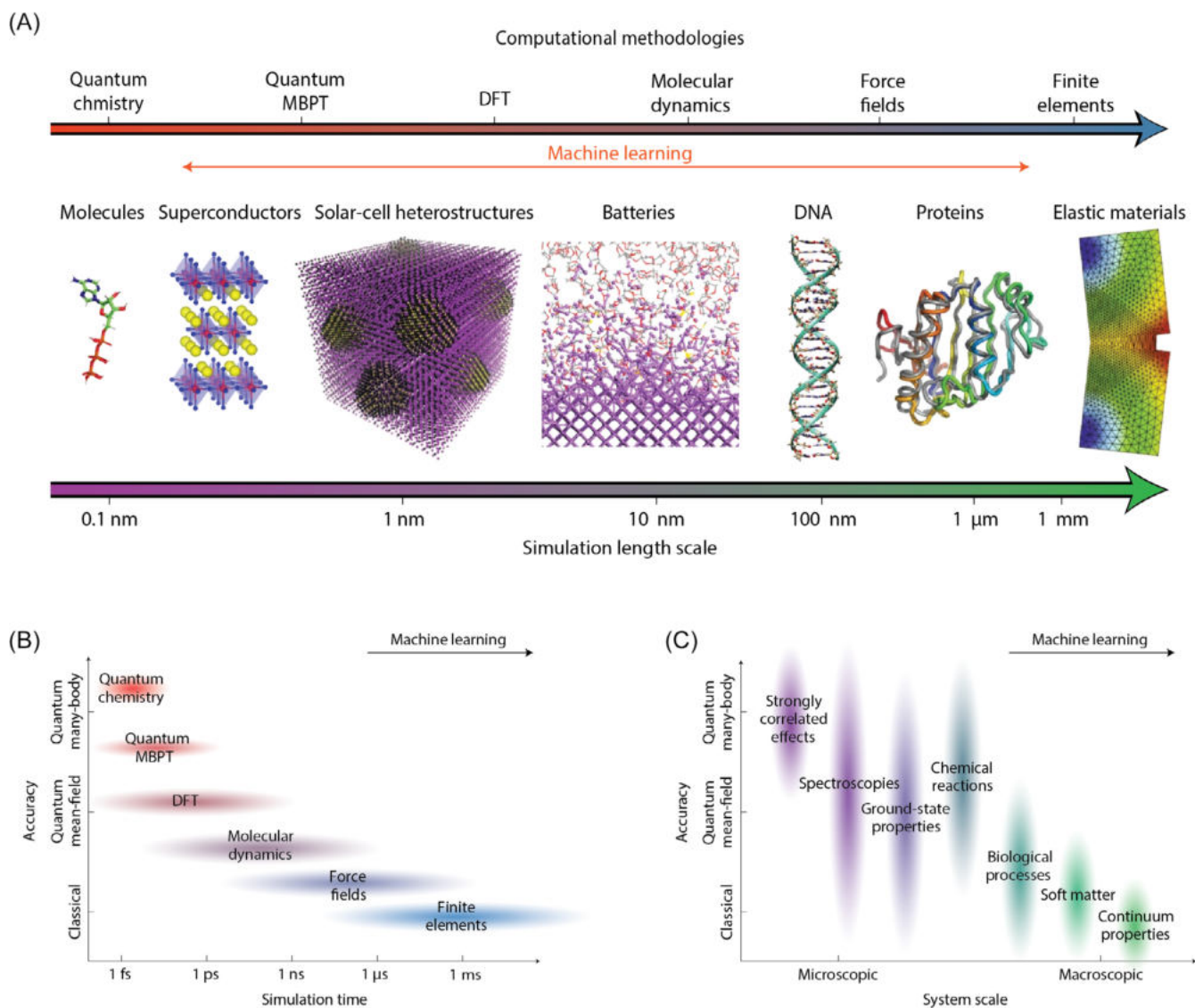


FIGURE 14 A bird's-eye view of computational materials science. (A) Contemporary quantum and classical computational methodologies address systems spanning from microscopic length scales (~ 0.1 nm) to macroscopic length scales (~ 1 mm). Examples of increasing length scales include an adenosine triphosphate (ATP) molecule, a high-temperature copper oxide superconductor, a heterostructure of perovskite solar cell and colloidal quantum dots, a metal–electrolyte interface in lithium batteries, a DNA structure, a structural model of a protein, and a simulated elastic material with propagating cracks. (B) Computational methods based on different levels of theory provide different accuracies. The achievable simulation time is usually bounded by the complexity and the accuracy of the theory required. (C) Different phenomena show up at different system scales, for which the level of theory varies depending on the nature of the problem. As indicated in (B) and (C), machine learning is expected to boost computational studies by improving simulation time and system size. *Source:* Reprinted with permission from Ref. [310], Springer Nature; solar cell heterostructures reprinted with permission from Ref. [311], Springer Nature Ltd; batteries from Ref. [312], ACS (batteries); DNA from Ref. [313], under a Creative Commons License CC BY 4.0; proteins from Ref. [314], Springer Nature Ltd; and elastic materials from Ref. [315], Elsevier.

powerful tools for a range of applications. These models are built on attention mechanisms and transformer architectures, with notable examples including generative pretrained transformer (GPT) models such as ChatGPT.³³⁶ Fine-tuned LLMs have been developed by training them on specialized corpora, such as research articles in the field of biological materials mechanics or textbooks focused on materials and multiscale methods, to accelerate progress

and discovery.^{337,338} Although these models occasionally produce errors and require significant alignment efforts, they have shown remarkable potential in identifying connections across diverse domains of knowledge and generating bioinspired design concepts.^{337,338}

Leveraging the AI-generated knowledge from natural organisms to drive material innovations—by designing compositions and structures that achieve similar or

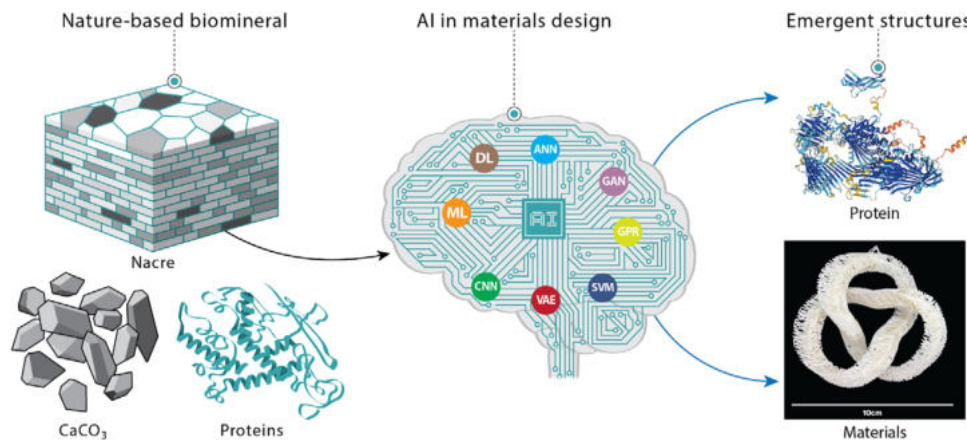


FIGURE 15 Left, a “brick-and-mortar” structure of nacre built of proteins and calcium carbonate (CaCO_3); middle, an illustration of artificial intelligence (AI) and the frequently used computational tools to enable materials discovery; right, vitellogenin protein and spider web–inspired structures. The structure of the vitellogenin protein—a precursor of egg yolk—as predicted by the AlphaFold tool.²⁷⁹ Source: Credit of protein: DeepMind; spider web structure reprinted with permission from Ref. [322], IOP Publishing.

superior performance to their counterparts—and producing them using advanced manufacturing techniques represents a significant frontier in materials science. Unsurprisingly, significant challenges remain. First of all, the type and quality of data, often derived from real-world studies by researchers, play a critical role in training AI models. The need for large amounts of accurate training data, informative representations that are independent of the system size, and accurate ML models remains an active research topic in the field.³³⁹ Additionally, the ability to integrate physical principles, reasoning logic, and algorithm development by scientists and engineers into AI is another key factor to drive progress in the field.³⁴⁰ For bioinspired materials in particular, utilizing AI to understand and optimize the interplay between different phases and architectures is essential to design novel hierarchical materials with enhanced performance characteristics, which may have potential for diverse applications in healthcare, energy, sustainability, and beyond.

5 | CONCLUSION AND FUTURE PERSPECTIVES

Nature’s hierarchical structures offer invaluable insights for the design of advanced materials with exceptional properties and multifunctionality, achieved with minimal energy and resources. This article has highlighted four notable examples: bone, nacre, sea sponge, and spider silk, illustrating their unique structural organization and resultant mechanical properties. Inspired by these natural models, researchers have made significant strides in developing bioinspired materials with applications in healthcare, energy storage, and sustainability. Advanced

manufacturing techniques, such as 3D printing and freeze casting, have enabled the creation of materials with hierarchical architectures, enhancing performance and functionality. Furthermore, the integration of AI in materials science could revolutionize the design and optimization of bioinspired materials, enabling the discovery of novel structures with superior properties.

There are numerous opportunities for significant breakthroughs in the field of nature-inspired materials, which hold the potential to address major human challenges. Here, we outline several frontiers in this domain:

1. **Fundamental understanding of natural organisms:** This involves gaining a thorough understanding of the growth, structure, and properties of natural organisms by employing a wide range of tools and techniques across various scientific disciplines. This includes advanced characterization techniques such as high-resolution microscopy, spectroscopy, and x-ray techniques; computational tools such as molecular dynamics simulations and bioinformatics; and analytical techniques like ML and multiscale modeling. These approaches will facilitate the establishment of robust composition–structure–property relationships in natural organisms.
2. **De novo design of proteins and inorganic materials:** Leveraging the power of AI tools to design novel proteins and inorganic materials is a key approach. Unlike natural organisms, synthetic materials are not constrained by available resources or processing conditions. This allows for the optimization of the balance between organic and inorganic components across multiple length scales and offers greater freedom in the selection of building blocks.

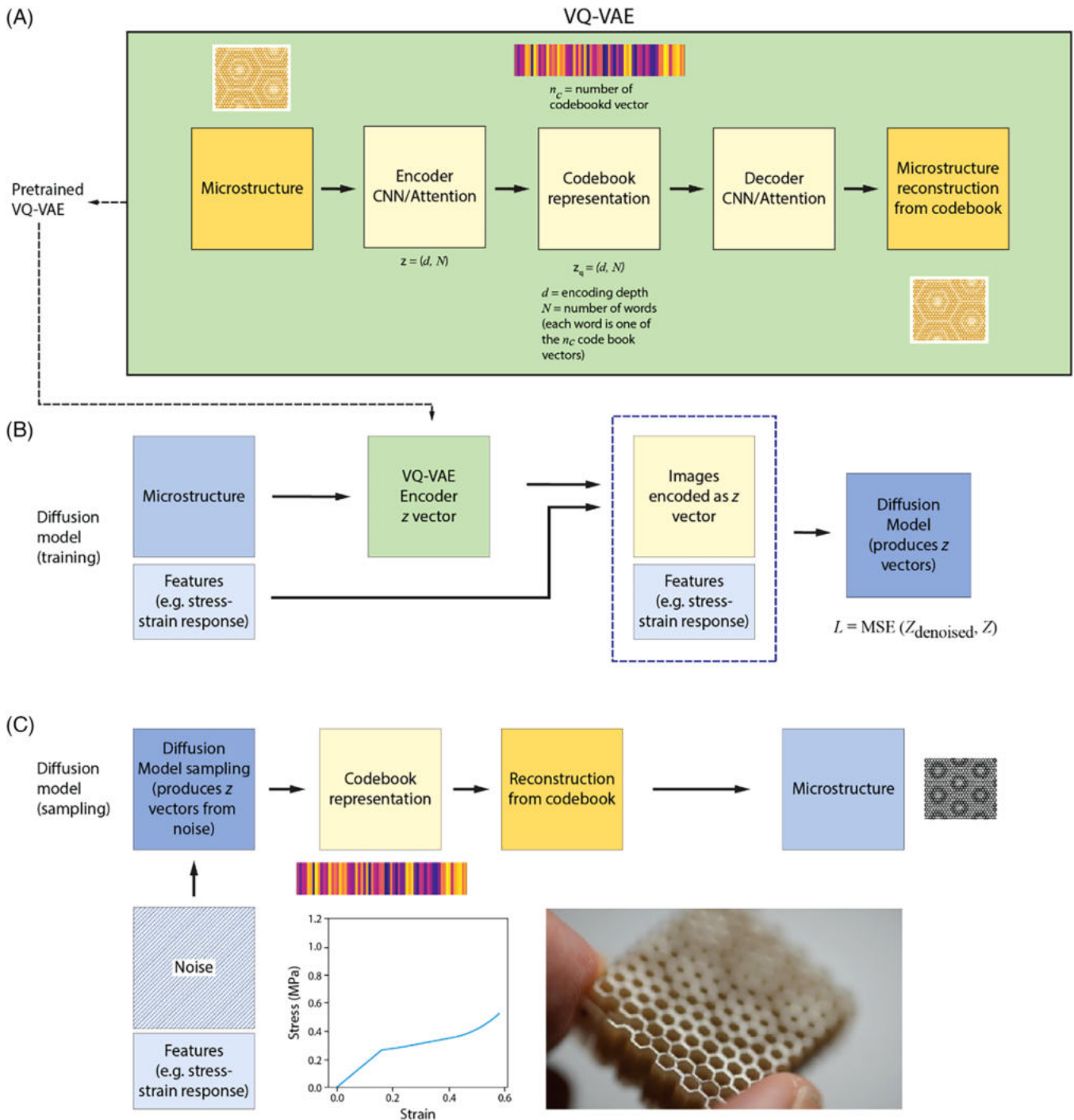


FIGURE 16 Overview of an integrated deep neural network architecture using (A) vector quantized variational autoencoder (VQ-VAE) model with (B, C) an attention-based diffusion model in the design of bioinspired hierarchical materials, and (D) an optical image of a three-dimensional (3D)-printed honeycomb resulting from the modeling. *Source:* Reprinted with permission from Ref. [328], IOP Publishing; honeycomb structure from Ref. [335], Elsevier.

3. Manufacturing of hierarchical structures: Employing advanced additive manufacturing or biomanufacturing processes to fabricate hierarchical structures awaits further research activities. Natural organisms exhibit hierarchical architecture down to molecular and nanometer levels, and achieving precise control

over synthetic materials at these length scales remains a formidable task. Moreover, the ability of biological materials to construct their complex structures using minimal, locally available resources—such as sugars, proteins, and minerals—and later recycle them as food or fertilizer through natural degradation offers

a compelling model for sustainable biomanufacturing practices by using materials that can be easily degraded.

4. **Enabling multifunctionality and self-healing in synthetic materials:** Developing man-made materials with multifunctional and self-healing capabilities is an exciting area of research. Natural organisms continuously rebuild and adapt to their local environments throughout their lifespans. Designing synthetic “living” materials with adaptive functionalities could extend the lifespan of engineering materials, thereby enhancing sustainability.

Interdisciplinary collaboration among materials scientists, biologists, engineers, and manufacturers is essential to overcome these technical challenges. Fortunately, recent progress in nanotechnology, biotechnology, and biomanufacturing holds significant potential to advance the field of materials science forward in the foreseeable future.

ACKNOWLEDGMENTS

Q.F. thanks Sarah Pakyala at Corning Inc., Peter Sucheski and Lisa Smith at Redstraw, LLC, for their help with the illustrations in Figures 4, 5, 7, and 15, and Yin Shu, Michael Badding, and Xingzhong Wu at Corning Inc. for helpful discussions.

DATA AVAILABILITY STATEMENT

The author has provided the required data availability statement and, if applicable, included functional and accurate links to said data therein.

ORCID

Qiang Fu  <https://orcid.org/0000-0001-9207-7715>

Francesco Baino  <https://orcid.org/0000-0001-8860-0497>

Hao Bai  <https://orcid.org/0000-0002-3348-6129>

John C. Mauro  <https://orcid.org/0000-0002-4319-3530>

REFERENCES

- Wegst UGK, Bai H, Saiz E, Tomsia AP, Ritchie RO. Bioinspired structural materials. *Nat Mater*. 2015;14(1):23–36.
- Chen P-Y, McKittrick J, Meyers MA. Biological materials: functional adaptations and bioinspired designs. *Prog Mater Sci*. 2012;57(8):1492–704.
- Fratzl P, Weinkamer R. Nature's hierarchical materials. *Prog Mater Sci*. 2007;52(8):1263–334.
- Heuer AH, Fink DJ, Larraia VJ, Arias JL, Calvert PD, Kendall K, et al. Innovative materials processing strategies: a biomimetic approach. *Science*. 1992;255(5048):1098–105.
- Eder M, Amini S, Fratzl P. Biological composites—complex structures for functional diversity. *Science*. 2018;362(6414):543–47.
- Cölfen H, Mann S. Higher-order organization by mesoscale self-assembly and transformation of hybrid nanostructures. *Angew Chem Int Ed*. 2003;42(21):2350–65.
- Mann S. *Biomaterialization: principles and concepts in bioinorganic materials chemistry*. New York: Oxford University Press; 2001.
- Meyers MA, Chen P-Y, Lin AY-M, Seki Y. Biological materials: structure and mechanical properties. *Prog Mater Sci*. 2008;53(1):1–206.
- Nepal D, Kang S, Adstedt KM, Kanhaiya K, Bockstaller MR, Brinson LC, et al. Hierarchically structured bioinspired nanocomposites. *Nat Mater*. 2023;22(1):18–35.
- Wagermaier W, Razghandi K, Fratzl P. A bio-inspired perspective on materials sustainability. *Adv Mater*. 2025;37(22):2413096.
- Meyers MA, McKittrick J, Chen P-Y. Structural biological materials: critical mechanics-materials connections. *Science*. 2013;339(6121):773–79.
- Lin A, Meyers MA. Growth and structure in abalone shell. *Mater Sci Eng A*. 2005;390(1):27–41.
- Yin Z, Hannard F, Barthelat F. Impact-resistant nacre-like transparent materials. *Science*. 2019;364(6447):1260–63.
- Fernandes MC, Aizenberg J, Weaver JC, Bertoldi K. Mechanically robust lattices inspired by deep-sea glass sponges. *Nat Mater*. 2021;20(2):237–41.
- Aizenberg J, Weaver JC, Thanawala MS, Sundar VC, Morse DE, Fratzl P. Skeleton of *Euplectella* sp.: structural hierarchy from the nanoscale to the macroscale. *Science*. 2005;309(5732):275–78.
- Weaver JC, Milliron GW, Allen P, Miserez A, Rawal A, Garay J, et al. Unifying design strategies in demosponge and hexactinellid skeletal systems. *J Adhes*. 2010;86(1):72–95.
- Baino F, Magnaterra G, Fiume E, Schiavi A, Tofan L-P, Schwentenwein M, et al. Digital light processing stereolithography of hydroxyapatite scaffolds with bone-like architecture, permeability, and mechanical properties. *J Am Ceram Soc*. 2022;105(3):1648–57.
- Chen G, Li W, Zhao B, Sun K. A novel biphasic bone scaffold: beta-calcium phosphate and amorphous calcium polyphosphate. *J Am Ceram Soc*. 2009;92(4):945–48.
- Deville S, Saiz E, Tomsia AP. Freeze casting of hydroxyapatite scaffolds for bone tissue engineering. *Biomaterials*. 2006;27(32):5480–89.
- Fu Q, Saiz E, Rahaman MN, Tomsia AP. Toward strong and tough glass and ceramic scaffolds for bone repair. *Adv Funct Mater*. 2013;23(44):5461–67.
- Fu Q, Saiz E, Tomsia AP. Bio-inspired highly porous and strong glass scaffolds. *Adv Funct Mater*. 2011;21:1058–63.
- Wagoner Johnson AJ, Herschler BA. A review of the mechanical behavior of CaP and CaP/polymer composites for applications in bone replacement and repair. *Acta Biomater*. 2011;7(1):16–30.
- Hutmacher DW. Scaffolds in tissue engineering bone and cartilage. *Biomaterials*. 2000;21(24):2529–43.
- Barthelat F. Growing a synthetic mollusk shell. *Science*. 2016;354(6308):32–33.
- Zhang X, Wu K, Ni Y, He L. Anomalous inapplicability of nacre-like architectures as impact-resistant templates in a wide range of impact velocities. *Nat Commun*. 2022;13(1):7719.

26. Li M, Zhao N, Wang M, Dai X, Bai H. Conch-shell-inspired tough ceramic. *Adv Funct Mater.* 2022;32(39):2205309.
27. Allmeling C, Jokuszies A, Reimers K, Kall S, Choi CY, Brandes G, et al. Spider silk fibres in artificial nerve constructs promote peripheral nerve regeneration. *Cell Prolif.* 2008;41(3):408–20.
28. Bandyopadhyay A, Chowdhury SK, Dey S, Moses JC, Mandal BB. Silk: a promising biomaterial opening new vistas towards affordable healthcare solutions. *J Indian Inst Sci.* 2019;99(3):445–87.
29. Dastagir K, Dastagir N, Limbourg A, Reimers K, Strauß S, Vogt PM. In vitro construction of artificial blood vessels using spider silk as a supporting matrix. *J Mech Behav Biomed Mater.* 2020;101:103436.
30. Pawar K, Welzel G, Haynl C, Schuster S, Scheibel T. Recombinant spider silk and collagen-based nerve guidance conduits support neuronal cell differentiation and functionality in vitro. *ACS Appl Bio Mater.* 2019;2(11):4872–80.
31. Wendt H, Hillmer A, Reimers K, Kuhbier JW, Schäfer-Nolte F, Allmeling C, et al. Artificial skin—culturing of different skin cell lines for generating an artificial skin substitute on cross-woven spider silk fibres. *PLoS ONE.* 2011;6(7):e21833.
32. Bixler GD, Bhushan B. Bioinspired rice leaf and butterfly wing surface structures combining shark skin and lotus effects. *Soft Matter.* 2012;8(44):11271–84.
33. Huynh T-P, Haick H. Learning from an intelligent mechanosensing system of plants. *Adv Mater Technol.* 2019;4(1):1800464.
34. Barthlott W, Neinhuis C. Purity of the sacred lotus, or escape from contamination in biological surfaces. *Planta.* 1997;202(1):1–8.
35. Nishimoto S, Bhushan B. Bioinspired self-cleaning surfaces with superhydrophobicity, superoleophobicity, and superhydrophilicity. *RSC Adv.* 2013;3(3):671–90.
36. Sun T, Feng L, Gao X, Jiang L. Bioinspired surfaces with special wettability. *Acc Chem Res.* 2005;38(8):644–52.
37. Fürstner R, Barthlott W, Neinhuis C, Walzel P. Wetting and self-cleaning properties of artificial superhydrophobic surfaces. *Langmuir.* 2005;21(3):956–61.
38. Wong T-S, Kang SH, Tang SKY, Smythe EJ, Hatton BD, Grinthal A, et al. Bioinspired self-repairing slippery surfaces with pressure-stable omniphobicity. *Nature.* 2011;477(7365):443–47.
39. Bhushan B, Jung YC. Natural and biomimetic artificial surfaces for superhydrophobicity, self-cleaning, low adhesion, and drag reduction. *Prog Mater Sci.* 2011;56(1):1–108.
40. Xu L, Geng Z, He J, Zhou G. Mechanically robust, thermally stable, broadband antireflective, and superhydrophobic thin films on glass substrates. *ACS Appl Mater Interfaces.* 2014;6(12):9029–35.
41. Woo S, Koh JH, Lee S, Yoon H, Char K. Trilevel-structured superhydrophobic pillar arrays with tunable optical functions. *Adv Funct Mater.* 2014;24(35):5550–56.
42. Teyssier J, Saenko SV, Van Der Marel D, Milinkovitch MC. Photonic crystals cause active colour change in chameleons. *Nat Commun.* 2015;6(1):6368.
43. Mähger LM, Denton EJ, Marshall NJ, Hanlon RT. Mechanisms and behavioural functions of structural coloration in cephalopods. *J R Soc, Interface.* 2009;6(Suppl2):S149–63.
44. Stuart-Fox D, Moussalli A. Camouflage, communication and thermoregulation: lessons from colour changing organisms. *Philos Trans R Soc B, Biol Sci.* 2009;364(1516):463–70.
45. Chou HH, Nguyen A, Chortos A, To JW, Lu C, Mei J. A chameleon-inspired stretchable electronic skin with interactive colour changing controlled by tactile sensing. *Nat Commun.* 2015;6:8011.
46. Larson C, Peele B, Li S, Robinson S, Totaro M, Beccai L, et al. Highly stretchable electroluminescent skin for optical signaling and tactile sensing. *Science.* 2016;351(6277):1071–74.
47. Vatankeh-Varnosfaderani M, Keith AN, Cong Y, Liang H, Rosenthal M, Sztucki M, et al. Chameleon-like elastomers with molecularly encoded strain-adaptive stiffening and coloration. *Science.* 2018;359(6383):1509–13.
48. Rus D, Tolley MT. Design, fabrication and control of soft robots. *Nature.* 2015;521(7553):467–75.
49. Fu F, Shang L, Chen Z, Yu Y, Zhao Y. Bioinspired living structural color hydrogels. *Sci Robot.* 2018;3(16):eaar8580.
50. Meyers MA, Lin AYM, Seki Y, Chen P-Y, Kad BK, Bodde S. Structural biological composites: an overview. *JOM.* 2006;58:35–41.
51. Wegst U, Ashby M. The mechanical efficiency of natural materials. *Philos Mag.* 2004;84(21):2167–86.
52. Ritchie RO. The conflicts between strength and toughness. *Nat Mater.* 2011;10(11):817–22.
53. Fung YC. *Biomechanics: mechanical properties of living tissues.* 2nd ed. New York: Springer-Verlag; 1993.
54. Fratzl P, Gupta HS, Paschalis EP, Roschger P. Structure and mechanical quality of the collagen-mineral nano-composite in bone. *J Mater Chem.* 2004;14(14):2115–23.
55. Athanasiou KA, Zhu C-F, Lanctot DR, Agrawal CM, Wang X. Fundamentals of biomechanics in tissue engineering of bone. *Tissue Eng.* 2000;6(4):361–81.
56. Weiner S, Wagner HD. The material bone: structure mechanical function relations. *Annu Rev Mater Sci.* 1998;28:271–98.
57. Launey ME, Buehler MJ, Ritchie RO. On the mechanistic origins of toughness in bone. *Annu Rev Mater Res.* 2010;40:25–53.
58. Keaveny TM, Hayes WC. Mechanical properties of cortical and trabecular bone. In: Hall BK, editors. *Bone: A Treatise.* Boca Raton, FL: CRC Press; 1993. p. 285–344.
59. Martin RB, Burr DB, Sharkey NA. *Skeletal tissue mechanics.* New York: Springer; 1998.
60. Reilly DT, Burstein AH, Frankel VH. Elastic-modulus for bone. *J Biomech.* 1974;7(3):271–72.
61. Rho JY, Hobatho MC, Ashman RB. Relations of mechanical-properties to density and ct numbers in human bone. *Med Eng Phys.* 1995;17(5):347–55.
62. Zioupos P, Currey JD. Changes in the stiffness, strength, and toughness of human cortical bone with age. *Bone.* 1998;22(1):57–66.
63. Bonfield W, Datta PK. Fracture toughness of compact bone. *J Biomech.* 1976;9(3):131–34.
64. Goldstein SA. The mechanical-properties of trabecular bone—dependence on anatomic location and function. *J Biomech.* 1987;20(11–12):1055–61.
65. Røhl L, Larsen E, Linde F, Odgaard A, Jørgensen J. Tensile and compressive properties of cancellous bone. *J Biomech.* 1991;24(12):1143–49.

66. Prakasam M, Locs J, Salma-Ancane K, Loca D, Largeteau A, Berzina-Cimdina L. Fabrication, properties and applications of dense hydroxyapatite: a review. *J Funct Biomater*. 2015;6(4):1099–140.
67. Hench LL. *Bioceramics*. *J Am Ceram Soc*. 1998;81(7):1705–28.
68. Nalla RK, Kinney JH, Ritchie RO. Mechanistic fracture criteria for the failure of human cortical bone. *Nat Mater*. 2003;2(3):164–68.
69. Currey JD, Sheppard PM. Mechanical properties of mother of pearl in tension. *Proc R Soc Lond Ser B Biol Sci*. 1977;196(1125):443–63.
70. Barthelat F, Tang H, Zavattieri P, Li C, Espinosa H. On the mechanics of mother-of-pearl: a key feature in the material hierarchical structure. *J Mech Phys Solids*. 2007;55(2):306–37.
71. Sarikaya M, Gunnison KE, Yasrebi M, Aksay IA. Mechanical property-microstructural relationships in abalone shell. *MRS Online Proc Lib*. 1989;174(1):109–16.
72. Menig R, Meyers MH, Meyers MA, Vecchio KS. Quasi-static and dynamic mechanical response of *Haliotis rufescens* (abalone) shells. *Acta Mater*. 2000;48(9):2383–98.
73. Jackson A, Vincent JF, Turner R. The mechanical design of nacre. *Proc R Soc London. Ser B. Boil Sci*. 1988;234(1277):415–40.
74. Barthelat F, Espinosa H. Elastic properties of nacre aragonite tablets. In *Proceedings of the 2003 SEM annual conference and exposition on experimental and applied mechanics*. Bethel, CT: Society for Experimental Mechanics; 2003.
75. Barthelat F, Li C-M, Comi C, Espinosa HD. Mechanical properties of nacre constituents and their impact on mechanical performance. *J Mater Res*. 2006;21(8):1977–86.
76. Ulian G, Valdrè G. Structural and elastic behaviour of aragonite at high-pressure: a contribution from first-principle simulations. *Comput Mater Sci*. 2022;212:111600.
77. Mayer G, Sarikaya M. Rigid biological composite materials: structural examples for biomimetic design. *Exp Mech*. 2002;42(4):395–403.
78. Sarikaya M, Fong H, Sunderland N, Flinn BD, Mayer G, Mescher A, et al. Biomimetic model of a sponge-spicular optical fiber—mechanical properties and structure. *J Mater Res*. 2001;16(5):1420–28.
79. Wang P, Yang F, Zheng B, Li P, Wang R, Li Y, et al. Breaking the tradeoffs between different mechanical properties in bioinspired hierarchical lattice metamaterials. *Adv Funct Mater*. 2023;33(45):2305978.
80. Heim M, Römer L, Scheibel T. Hierarchical structures made of proteins. The complex architecture of spider webs and their constituent silk proteins. *Chem Soc Rev*. 2010;39(1):156–64.
81. Eisdoldt L, Smith A, Scheibel T. Decoding the secrets of spider silk. *Mater Today*. 2011;14(3):80–86.
82. Gosline JM, Guerette PA, Ortlepp CS, Savage KN. The mechanical design of spider silks: from fibroin sequence to mechanical function. *J Exp Biol*. 1999;202(23):3295–303.
83. Keten S, Xu Z, Ihle B, Buehler MJ. Nanoconfinement controls stiffness, strength and mechanical toughness of β -sheet crystals in silk. *Nat Mater*. 2010;9(4):359–67.
84. Van Beek JD, Hess S, Vollrath F, Meier BH. The molecular structure of spider dragline silk: folding and orientation of the protein backbone. *Proc Natl Acad Sci*. 2002;99(16):10266–71.
85. Thiel BL, Guess KB, Viney C. Non-periodic lattice crystals in the hierarchical microstructure of spider (major ampullate) silk. *Biopolymers: Orig Res Biomolecules*. 1997;41(7):703–19.
86. Hayashi CY, Shipley NH, Lewis RV. Hypotheses that correlate the sequence, structure, and mechanical properties of spider silk proteins. *Int J Biol Macromol*. 1999;24(2–3):271–75.
87. Blackledge TA, Hayashi CY. Silken toolkits: biomechanics of silk fibers spun by the orb web spider *Argiope argentata* (Fabricius 1775). *J Exp Biol*. 2006;209(13):2452–61.
88. Denny M. The physical properties of spider's silk and their role in the design of orb-webs. *J Exp Biol*. 1976;65(2):483–506.
89. Vincent JFV, Bogatyreva OA, Bogatyrev NR, Bowyer A, Pahl A-K. Biomimetics: its practice and theory. *J R Soc Interface*. 2006;3(9):471–82.
90. Persidis A. Tissue engineering. *Nat Biotechnol*. 1999;17(5):508–10.
91. Boyce T, Edwards J, Scarborough N. Allograft bone—the influence of processing on safety and performance. *Orthop Clin North Am*. 1999;30(4):571–81.
92. Van Heest A, Swiontkowski M. Bone-graft substitutes. *Lancet*. 1999;353:SI28–SI29.
93. William Jr, G, Einhorn TA, Koval K, McKee M, Smith W, Sanders R, et al. Bone grafts and bone graft substitutes in orthopaedic trauma surgery: a critical analysis. *J Bone Joint Surg Am*. 2007;89(3):649–58.
94. Agrawal CM, Ray RB. Biodegradable polymeric scaffolds for musculoskeletal tissue engineering. *J Biomed Mater Res*. 2001;55(2):141–50.
95. Griffith LG. Polymeric biomaterials. *Acta Mater*. 2000;48(1):263–77.
96. Hayashi T. Biodegradable polymers for biomedical uses. *Prog Polym Sci*. 1994;19(4):663–702.
97. Lee KY, Mooney DJ. Hydrogels for tissue engineering. *Chem Rev*. 2001;101(7):1869–79.
98. LeGeros RZ. Biodegradation and bioresorption of calcium phosphate ceramics. *Clin Mater*. 1993;14(1):65–88.
99. Dorozhkin SV. Bioceramics of calcium orthophosphates. *Biomaterials*. 2010;31(7):1465–85.
100. Dorozhkin SV. Biphasic, triphasic and multiphasic calcium orthophosphates. *Acta Biomater*. 2012;8(3):963–77.
101. Rahaman MN, Day DE, Sonny Bal B, Fu Q, Jung SB, Bonewald LF, et al. Bioactive glass in tissue engineering. *Acta Biomater*. 2011;7(6):2355–73.
102. Brauer DS. Bioactive glasses—structure and properties. *Angew Chem Int Ed*. 2015;54(14):4160–81.
103. Hench LL, Paschall H. Direct chemical bond of bioactive glass-ceramic materials to bone and muscle. *J Biomed Mater Res*. 1973;7(3):25–42.
104. Hench LL, Polak JM. Third-generation Biomedical materials. *Science*. 2002;295(5557):1014–17.
105. Hench LL, Wilson J. Surface-active biomaterials. *Science*. 1984;226(4675):630–36.
106. Kokubo T. Bioactive glass ceramics: properties and applications. *Biomaterials*. 1991;12(2):155–63.
107. Kokubo T. Surface chemistry of bioactive glass-ceramics. *J Non-Cryst Solids*. 1990;120(1–3):138–51.
108. Cresswell-Boyes AJ, Davis GR, Krishnamoorthy M, Mills D, Barber AH. Composite 3D printing of biomimetic human teeth. *Sci Rep*. 2022;12(1):7830.

109. Apel E, Deubener J, Bernard A, Höland M, Müller R, Kappert H, et al. Phenomena and mechanisms of crack propagation in glass-ceramics. *J Mech Behav Biomed Mater*. 2008;1(4):313–25.
110. Gillam DG, Tang JY, Mordan NJ, Newman HN. The effects of a novel Bioglass® dentifrice on dentine sensitivity: a scanning electron microscopy investigation. *J Oral Rehabil*. 2002;29(4):305–13.
111. Fu Q, Beall GH, Smith CM. Nature-inspired design of strong, tough glass-ceramics. *MRS Bull*. 2017;42(3):220–25.
112. Langer R, Vacanti JP. Tissue engineering. *Science*. 1993;260(5110):920–26.
113. Nerem RM. Cellular engineering. *Ann Biomed Eng*. 1991;19(5):529–45.
114. Hoppe A, Güldal NS, Boccaccini AR. A review of the biological response to ionic dissolution products from bioactive glasses and glass-ceramics. *Biomaterials*. 2011;32(11):2757–74.
115. Fu Q, Saiz E, Tomsia AP. Direct ink writing of highly porous and strong glass scaffolds for load-bearing bone defects repair and regeneration. *Acta Biomater*. 2011;7(10):3547–54.
116. Jia W, Lau GY, Huang W, Zhang C, Tomsia AP, Fu Q. Bioactive glass for large bone repair. *Adv Healthc Mater*. 2015;4(18):2842–48.
117. Baino F, Schwentenwein M, Verné E. Modelling the mechanical properties of hydroxyapatite scaffolds produced by digital light processing-based vat photopolymerization. *Ceramics*. 2022;5(3):593–600.
118. Baino F, Dias J, Alidoost M, Schwentenwein M, Verné E. Making foam-like bioactive glass scaffolds by vat photopolymerization. *Open Ceram*. 2023;15:100392.
119. Baino F, Gaido F, Gabrieli R, Alidoost D, Schiavi A, Mohammadi M, et al. Vat photopolymerization of ultra-porous bioactive glass foams. *Open Ceram*. 2024;20:100690.
120. Maevskaia E, Khera N, Ghayor C, Bhattacharya I, Guerrero J, Nicholls F, et al. Three-dimensional printed hydroxyapatite bone substitutes designed by a novel periodic minimal surface algorithm are highly osteoconductive. *3D Print Addit Manuf*. 2023;10(5):905–16.
121. Wang Y, Liu Y, Chen S, Francis Siu M-F, Liu C, Bai J, et al. Enhancing bone regeneration through 3D printed biphasic calcium phosphate scaffolds featuring graded pore sizes. *Bioact Mater*. 2025;46:21–36.
122. Deville S, Saiz E, Nalla RK, Tomsia AP. Freezing as a path to build complex composites. *Science*. 2006;311(5760):515–18.
123. Liu X, Rahaman MN, Fu QA. Oriented bioactive glass (13-93) scaffolds with controllable pore size by unidirectional freezing of camphene-based suspensions: microstructure and mechanical response. *Acta Biomater*. 2011;7(1):406–16.
124. Fu Q, Rahaman MN, Bal BS, Brown RF. Preparation and in vitro evaluation of bioactive glass (13-93) scaffolds with oriented microstructures for repair and regeneration of load-bearing bones. *J Biomed Mater Res A*. 2010;93A(4):1380–90.
125. Fu Q, Rahaman MN, Dogan F, Bal BS. Freeze casting of porous hydroxyapatite scaffolds. I. Processing and general microstructure. *J Biomed Mater Res B Appl Biomater*. 2008;86B(1):125–35.
126. Baino F, Ferraris M. Learning from Nature: using bioinspired approaches and natural materials to make porous bioceramics. *Int J Appl Ceram Technol*. 2017;14(4):507–20.
127. Fu Q, Aaldenberg EM, Coon EN, Gross TM, Whittier AM, Abel BM, et al. Tough, bioinspired transparent glass-ceramics. *Adv Eng Mater*. 2022;24(9):2200350.
128. Fu Q, Jia W, Lau GY, Tomsia AP. Strength, toughness, and reliability of a porous glass/biopolymer composite scaffold. *J Biomed Mater Res B Appl Biomater*. 2018;106(3):1209–17.
129. Baoyong L, Jian Z, Denglong C, Min L. Evaluation of a new type of wound dressing made from recombinant spider silk protein using rat models. *Burns*. 2010;36(6):891–96.
130. Gomes S, Leonor IB, Mano JF, Reis RL, Kaplan DL. Spider silk-bone sialoprotein fusion proteins for bone tissue engineering. *Soft Matter*. 2011;7(10):4964–73.
131. Su X, Wei L, Xu Z, Qin L, Yang J, Zou Y, et al. Evaluation and application of silk fibroin based biomaterials to promote cartilage regeneration in osteoarthritis therapy. *Biomedicines*. 2023;11(8):2244.
132. Johansson U, Widhe M, Shalaly ND, Arregui IL, Nilebäck L, Tasiopoulos CP, et al. Assembly of functionalized silk together with cells to obtain proliferative 3D cultures integrated in a network of ECM-like microfibers. *Sci Rep*. 2019;9(1):6291.
133. Thurber AE, Omenetto FG, Kaplan DL. In vivo bioresponses to silk proteins. *Biomaterials*. 2015;71:145–57.
134. Helfricht N, Klug M, Mark A, Kuznetsov V, Blüm C, Scheibel T, et al. Surface properties of spider silk particles in solution. *Biomater Sci*. 2013;1(11):1166–71.
135. Florczak A, Jastrzebska K, Mackiewicz A, Dams-Kozłowska H. Blending two bioengineered spider silks to develop cancer targeting spheres. *J Mater Chem B*. 2017;5(16):3000–3011.
136. Cao B, Mao C. Oriented nucleation of hydroxylapatite crystals on spider dragline silks. *Langmuir*. 2007;23(21):10701–5.
137. Dellaquila A, Greco G, Campodoni E, Mazzocchi M, Mazzolai B, Tampieri A, et al. Optimized production of a high-performance hybrid biomaterial: biomineralized spider silk for bone tissue engineering. *J Appl Polym Sci*. 2020;137(22):48739.
138. Neubauer VJ, Scheibel T. Spider silk fusion proteins for controlled collagen binding and biomineralization. *ACS Biomater Sci Eng*. 2020;6(10):5599–608.
139. Rising A, Johansson J. Toward spinning artificial spider silk. *Nat Chem Biol*. 2015;11(5):309–15.
140. Kang K, Meng YS, Bréger J, Grey CP, Ceder G. Electrodes with high power and high capacity for rechargeable lithium batteries. *Science*. 2006;311(5763):977–80.
141. Chiang Y-M. Building a better battery. *Science*. 2010;330(6010):1485–86.
142. Augustyn V, Come J, Lowe MA, Kim JW, Taberna P-L, Tolbert SH, et al. High-rate electrochemical energy storage through Li⁺ intercalation pseudocapacitance. *Nat Mater*. 2013;12(6):518–22.
143. Lin M-C, Gong M, Lu B, Wu Y, Wang D-Y, Guan M, et al. An ultrafast rechargeable aluminium-ion battery. *Nature*. 2015;520(7547):324–28.
144. Simon P, Gogotsi Y. Materials for electrochemical capacitors. *Nat Mater*. 2008;7(11):845–54.
145. Aricò AS, Bruce P, Scrosati B, Tarascon J-M, Van Schalkwijk W. Nanostructured materials for advanced energy conversion and storage devices. *Nat Mater*. 2005;4(5):366–77.
146. Anasori B, Lukatskaya MR, Gogotsi Y. 2D metal carbides and nitrides (MXenes) for energy storage. In *MXenes*. New Delhi: Jenny Stanford Publishing; 2023. p. 677–722.

147. Bruce PG, Freunberger SA, Hardwick LJ, Tarascon J-M. Li-O₂ and Li-S batteries with high energy storage. *Nat Mater*. 2012;11(1):19–29.
148. Goodenough JB, Kim Y. Challenges for rechargeable Li batteries. *Chem Mater*. 2010;22(3):587–603.
149. Goodenough JB, Park K-S. The Li-ion rechargeable battery: a perspective. *J Am Chem Soc*. 2013;135(4):1167–76.
150. Winter M, Brodd RJ. What are batteries, fuel cells, and supercapacitors? *Chem Rev*. 2004;104(10):4245–70.
151. Goodenough JB, Mizushima K, Wiseman PJ. Electrochemical cell and method of making ion conductors for said cell. Shoreham-by-Sea: Ricardo AEA Ltd; 1984.
152. Mizushima K, Jones P, Wiseman P, Goodenough J. Li_xCoO₂ (0 < x < 1): a new cathode material for batteries of high energy density. *Mater Res Bull*. 1980;15(6):783–89.
153. Whittingham MS. Chalcogenide battery. Spring, TX: Exxon-Mobil Technology and Engineering Co; 1976.
154. Whittingham MS. Electrical energy storage and intercalation chemistry. *Science*. 1976;192(4244):1126–27.
155. Whittingham MS, Gamble FR. The lithium intercalates of the transition metal dichalcogenides. *Mater Res Bull*. 1975;10(5):363–71.
156. Whittingham MS. Electrointercalation in transition-metal disulphides. *J Chem Soc, Chem Commun*. 1974;9:328–29.
157. Goodenough JB, Mizushima K. Fast ion conductors. Shoreham-by-Sea: Ricardo AEA Ltd; 1982.
158. Yoshino A, Sanekika K, Nakajima T. Secondary battery. Tokyo: Asahi Kasei Corp; 1987.
159. Goodenough JB. How we made the Li-ion rechargeable battery. *Nat Electron*. 2018;1(3):204–204.
160. Kaskhedikar NA, Maier J. Lithium storage in carbon nanostructures. *Adv Mater*. 2009;21(25–26):2664–80.
161. Etacheri V, Marom R, Elazari R, Salitra G, Aurbach D. Challenges in the development of advanced Li-ion batteries: a review. *Energy Environ Sci*. 2011;4(9):3243–62.
162. Li Y, Lu Y, Adelhelm P, Titirici M-M, Hu Y-S. Intercalation chemistry of graphite: alkali metal ions and beyond. *Chem Soc Rev*. 2019;48(17):4655–87.
163. Yu P, Popov BN, Ritter JA, White RE. Determination of the lithium ion diffusion coefficient in graphite. *J Electrochem Soc*. 1999;146(1):8.
164. Manthiram A. An outlook on lithium ion battery technology. *ACS Cent Sci*. 2017;3(10):1063–69.
165. Sandhya C, John B, Gouri C. Lithium titanate as anode material for lithium-ion cells: a review. *Ionics*. 2014;20:601–20.
166. Oumellal Y, Delpuech N, Mazouzi D, Dupré N, Gaubicher J, Moreau P, et al. The failure mechanism of nano-sized Si-based negative electrodes for lithium ion batteries. *J Mater Chem*. 2011;21(17):6201–8.
167. Meister P, Jia H, Li J, Kloepsch R, Winter M, Placke T. Best practice: performance and cost evaluation of lithium ion battery active materials with special emphasis on energy efficiency. *Chem Mater*. 2016;28(20):7203–17.
168. Tarascon JM, Armand M. Issues and challenges facing rechargeable lithium batteries. *Nature*. 2001;414(6861):359–67.
169. Liu J, Bao Z, Cui Y, Dufek EJ, Goodenough JB, Khalifah P, et al. Pathways for practical high-energy long-cycling lithium metal batteries. *Nat Energy*. 2019;4(3):180–86.
170. Idota Y, Kubota T, Matsufuji A, Maekawa Y, Miyasaka T. Tin-based amorphous oxide: a high-capacity lithium-ion-storage material. *Science*. 1997;276(5317):1395–97.
171. Paek S-M, Yoo E, Honma I. Enhanced cyclic performance and lithium storage capacity of SnO₂/graphene nanoporous electrodes with three-dimensionally delaminated flexible structure. *Nano Lett*. 2009;9(1):72–75.
172. Padhi AK, Nanjundaswamy KS, Goodenough JB. Phospholivines as positive-electrode materials for rechargeable lithium batteries. *J Electrochem Soc*. 1997;144(4):1188.
173. Thackeray MM, David WIF, Bruce PG, Goodenough JB. Lithium insertion into manganese spinels. *Mater Res Bull*. 1983;18(4):461–72.
174. Wang L, Chen B, Ma J, Cui G, Chen L. Reviving lithium cobalt oxide-based lithium secondary batteries-toward a higher energy density. *Chem Soc Rev*. 2018;47(17):6505–602.
175. Manthiram A. Materials challenges and opportunities of lithium ion batteries. *J Phys Chem Lett*. 2011;2(3):176–84.
176. Evro S, Ajumobi A, Mayon D, Tomomewo OS. Navigating battery choices: a comparative study of lithium iron phosphate and nickel manganese cobalt battery technologies. *Future Batteries*. 2024;4:100007.
177. Cheng AL, Fuchs ERH, Karplus VJ, Michalek JJ. Electric vehicle battery chemistry affects supply chain disruption vulnerabilities. *Nat Commun*. 2024;15(1):2143.
178. Ma R, Tao S, Sun X, Ren Y, Sun C, Ji G, et al. Pathway decisions for reuse and recycling of retired lithium-ion batteries considering economic and environmental functions. *Nat Commun*. 2024;15(1):7641.
179. Li W, Erickson EM, Manthiram A. High-nickel layered oxide cathodes for lithium-based automotive batteries. *Nat Energy*. 2020;5(1):26–34.
180. Cheng H-M, Li F. Charge delivery goes the distance. *Science*. 2017;356(6338):582–83.
181. Sun H, Mei L, Liang J, Zhao Z, Lee C, Fei H, et al. Three-dimensional holey-graphene/niobia composite architectures for ultrahigh-rate energy storage. *Science*. 2017;356(6338):599–604.
182. Sun H, Zhu J, Baumann D, Peng L, Xu Y, Shakir I, et al. Hierarchical 3D electrodes for electrochemical energy storage. *Nat Rev Mater*. 2019;4(1):45–60.
183. Wang Y, Song J, Huang L, Xu L, Xu H, Zhu J, et al. Bioinspired hierarchical porous architecture for enhanced kinetics and mechanical integrity in thick cathode. *Small*. 2024;20(52):2406058.
184. Sun K, Wei T-S, Ahn BY, Seo JY, Dillon SJ, Lewis JA. 3D Printing of interdigitated Li-ion microbattery architectures. *Adv Mater*. 2013;25(33):4539–43.
185. Wei T-S, Ahn BY, Grotto J, Lewis JA. 3D Printing of customized Li-ion batteries with thick electrodes. *Adv Mater*. 2018;30(16):1703027.
186. Cao D, Xing Y, Tantratrian K, Wang X, Ma Y, Mukhopadhyay A, et al. 3D Printed high-performance lithium metal microbatteries enabled by nanocellulose. *Adv Mater*. 2019;31(14):1807313.
187. Fu K, Wang Y, Yan C, Yao Y, Chen Y, Dai J, et al. Graphene oxide-based electrode inks for 3D-printed lithium-ion batteries. *Adv Mater*. 2016;28(13):2587–94.

188. Wang Y, Chen C, Xie H, Gao T, Yao Y, Pastel G, et al. 3D-Printed all-Fiber Li-ion battery toward wearable energy storage. *Adv Funct Mater.* 2017;27(43):1703140.
189. Lacey SD, Kirsch DJ, Li Y, Morgenstern JT, Zarket BC, Yao Y, et al. Extrusion-based 3D printing of hierarchically porous advanced battery electrodes. *Adv Mater.* 2018;30(12):1705651.
190. Delattre B, Amin R, Sander J, De Coninck J, Tomsia AP, Chiang Y-M. Impact of pore tortuosity on electrode kinetics in lithium battery electrodes: study in directionally freeze-cast LiNiO. 8CoO. 15AlO. 05O2 (NCA). *J Electrochem Soc.* 2018;165(2):A388–95.
191. Choi D, Choy KL. Spider silk binder for Si-based anode in lithium-ion batteries. *Mater Des.* 2020;191:108669.
192. Wang Y, Zhu J, Chen A, Guo X, Cui H, Chen Z, et al. Spider silk-inspired binder design for flexible lithium-ion battery with high durability. *Adv Mater.* 2023;35(47):2303165.
193. Kato Y, Hori S, Saito T, Suzuki K, Hirayama M, Mitsui A, et al. High-power all-solid-state batteries using sulfide superionic conductors. *Nat Energy.* 2016;1(4):1–7.
194. Famprikis T, Canepa P, Dawson JA, Islam MS, Masquelier C. Fundamentals of inorganic solid-state electrolytes for batteries. *Nat Mater.* 2019;18(12):1278–91.
195. Randau S, Weber DA, Kötz O, Koerver R, Braun P, Weber A, et al. Benchmarking the performance of all-solid-state lithium batteries. *Nat Energy.* 2020;5(3):259–70.
196. Wang H, Ozkan CS, Zhu H, Li X. Advances in solid-state batteries: materials, interfaces, characterizations, and devices. *MRS Bull.* 2023;48(12):1221–29.
197. Janek J, Zeier WG. Challenges in speeding up solid-state battery development. *Nat Energy.* 2023;8(3):230–40.
198. Sau K, Takagi S, Ikeshoji T, Kisu K, Sato R, Dos Santos EC, et al. Unlocking the secrets of ideal fast ion conductors for all-solid-state batteries. *Commun Mater.* 2024;5(1):122.
199. Wang T, Chen B, Liu Y, Song Z, Wang Z, Chen Y, et al. Fatigue of Li metal anode in solid-state batteries. *Science.* 2025;388(6744):311–16.
200. Manthiram A, Yu X, Wang S. Lithium battery chemistries enabled by solid-state electrolytes. *Nat Rev Mater.* 2017;2(4):1–16.
201. Kamaya N, Homma K, Yamakawa Y, Hirayama M, Kanno R, Yonemura M, et al. A lithium superionic conductor. *Nat Mater.* 2011;10(9):682–86.
202. Bates AM, Preger Y, Torres-Castro L, Harrison KL, Harris SJ, Hewson J. Are solid-state batteries safer than lithium-ion batteries? *Joule.* 2022;6(4):742–55.
203. Li J, Ma C, Chi M, Liang C, Dudney NJ. Solid electrolyte: the key for high-voltage lithium batteries. *Adv Energy Mater.* 2015;5(4):1401408.
204. Janek J, Zeier WG. A solid future for battery development. *Nat Energy.* 2016;1(9):1–4.
205. Albertus P, Babinec S, Litzelman S, Newman A. Status and challenges in enabling the lithium metal electrode for high-energy and low-cost rechargeable batteries. *Nat Energy.* 2018;3(1):16–21.
206. Tan DHS, Chen Y-T, Yang H, Bao W, Sreenarayanan B, Doux J-M, et al. Carbon-free high-loading silicon anodes enabled by sulfide solid electrolytes. *Science.* 2021;373(6562):1494–99.
207. Quartarone E, Mustarelli P. Electrolytes for solid-state lithium rechargeable batteries: recent advances and perspectives. *Chem Soc Rev.* 2011;40(5):2525–40.
208. Hu Y-S. Batteries: getting solid. *Nat Energy.* 2016;1(4):1–2.
209. Fergus JW. Ceramic and polymeric solid electrolytes for lithium-ion batteries. *J Power Sources.* 2010;195(15):4554–69.
210. Xia W, Xu B, Duan H, Guo Y, Kang H, Li H, et al. Ionic conductivity and air stability of Al-doped Li₇La₃Zr₂O₁₂ sintered in alumina and Pt crucibles. *ACS Appl Mater Interfaces.* 2016;8(8):5335–42.
211. Fan L, Wei S, Li S, Li Q, Lu Y. Recent progress of the solid-state electrolytes for high-energy metal-based batteries. *Adv Energy Mater.* 2018;8(11):1702657.
212. Fu J. Fast Li⁺ ion conducting glass-ceramics in the system Li₂O–Al₂O₃–GeO₂–P₂O₅. *Solid State Ionics.* 1997;104(3–4):191–94.
213. Cheng Q, Li A, Li N, Li S, Zangiabadi A, Li T-D, et al. Stabilizing solid electrolyte-anode interface in Li-metal batteries by boron nitride-based nanocomposite coating. *Joule.* 2019;3(6):1510–22.
214. Aono H, Sugimoto E, Sadaoka Y, Imanaka N, Adachi G-Y. Ionic conductivity of solid electrolytes based on lithium titanium phosphate. *J Electrochem Soc.* 1990;137(4):1023.
215. Han F, Zhu Y, He X, Mo Y, Wang C. Electrochemical stability of Li₁₀GeP₂S₁₂ and Li₇La₃Zr₂O₁₂ solid electrolytes. *Adv Energy Mater.* 2016;6(8):1501590.
216. Chi S-S, Liu Y, Zhao N, Guo X, Nan C-W, Fan L-Z. Solid polymer electrolyte soft interface layer with 3D lithium anode for all-solid-state lithium batteries. *Energy Stor Mater.* 2019;17:309–16.
217. Mizuno F, Hayashi A, Tadanaga K, Tatsumisago M. New, highly ion-conductive crystals precipitated from Li₂SP₂S₃ glasses. *Adv Mater (Weinheim).* 2005;17:918–21.
218. Bates JB, Dudney NJ, Gruzalski GR, Zuhr RA, Choudhury A, Luck CF, et al. Fabrication and characterization of amorphous lithium electrolyte thin films and rechargeable thin-film batteries. *J Power Sources.* 1993;43(1–3):103–10.
219. Bates J, Dudney NJ, Neudecker B, Ueda A, Evans CD. Thin-film lithium and lithium-ion batteries. *Solid State Ionics.* 2000;135(1–4):33–45.
220. Xue Z, He D, Xie X. Poly (ethylene oxide)-based electrolytes for lithium-ion batteries. *J Mater Chem A.* 2015;3(38):19218–53.
221. Croce F, Appetecchi GB, Persi L, Scrosati B. Nanocomposite polymer electrolytes for lithium batteries. *Nature.* 1998;394(6692):456–58.
222. Deng Z, Wang Z, Chu I-H, Luo J, Ong SP. Elastic properties of alkali superionic conductor electrolytes from first principles calculations. *J Electrochem Soc.* 2015;163(2):A67.
223. Yu S, Schmidt RD, Garcia-Mendez R, Herbert E, Dudney NJ, Wolfenstine JB, et al. Elastic properties of the solid electrolyte Li₇La₃Zr₂O₁₂ (LLZO). *Chem Mater.* 2016;28(1):197–206.
224. Li A, Liao X, Zhang H, Shi L, Wang P, Cheng Q, et al. Nacre-inspired composite electrolytes for load-bearing solid-state lithium-metal batteries. *Adv Mater.* 2020;32(2):1905517.
225. Yi E, Shen H, Heywood S, Alvarado J, Parkinson DY, Chen G, et al. All-solid-state batteries using rationally designed garnet electrolyte frameworks. *ACS Appl Energy Mater.* 2020;3(1):170–75.
226. Pachauri RK, Allen MR, Barros VR, Broome J, Cramer W, Christ R, et al. Climate change 2014: synthesis report. *Contribu-*

- tion of working groups I, II and III to the fifth assessment report of the Intergovernmental Panel on Climate Change. Geneva: IPCC; 2014.
227. Union U. Report of the world commission on environment and development: our common future. 1987 [cited 2025 Jan 30]. Available from: <http://www.un-documents.net/wced-ocf.htm>
 228. Ellen MacArthur Foundation. The butterfly diagram: visualising the circular economy. 2021 [cited 2025 Jan 30]. Available from: www.ellenmacarthurfoundation.org
 229. Olivetti EA, Cullen JM. Toward a sustainable materials system. *Science*. 2018;360(6396):1396–98.
 230. Mohanty AK, Vivekanandhan S, Pin J-M, Misra M. Composites from renewable and sustainable resources: challenges and innovations. *Science*. 2018;362(6414):536–42.
 231. Ding Y, Pang Z, Lan K, Yao Y, Panzarasa G, Xu L, et al. Emerging engineered wood for building applications. *Chem Rev*. 2023;123(5):1843–88.
 232. Rising A, Harrington MJ. Biological materials processing: time-tested tricks for sustainable fiber fabrication. *Chem Rev*. 2023;123(5):2155–99.
 233. Chen H, Simoska O, Lim K, Grattieri M, Yuan M, Dong F, et al. Fundamentals, applications, and future directions of bioelectrocatalysis. *Chem Rev*. 2020;120(23):12903–93.
 234. Chen H, Dong F, Minter SD. The progress and outlook of bioelectrocatalysis for the production of chemicals, fuels and materials. *Nat Catal*. 2020;3(3):225–44.
 235. Freguia S, Viridis B, Harnisch F, Keller J. Bioelectrochemical systems: microbial versus enzymatic catalysis. *Electrochim Acta*. 2012;82:165–74.
 236. Cadoux C, Milton R. Recent enzymatic electrochemistry for reductive reactions. *ChemElectroChem*. 2020;7:1974–86.
 237. Guo J, Suástegui M, Sakimoto KK, Moody VM, Xiao G, Nocera DG, et al. Light-driven fine chemical production in yeast biohybrids. *Science*. 2018;362(6416):813–16.
 238. Guan X, Erşan S, Xie Y, Park J, Liu C. Redox and energy homeostasis enabled by photocatalytic material–microbial interfaces. *ACS Nano*. 2024;18(31):20567–75.
 239. An B, Wang Y, Huang Y, Wang X, Liu Y, Xun D, et al. Engineered living materials for sustainability. *Chem Rev*. 2023;123(5):2349–419.
 240. Hager MD, Greil P, Leyens C, Van Der Zwaag S, Schubert US. Self-healing materials. *Adv Mater*. 2010;22(47):5424–30.
 241. De Belie N, Gruyaert E, Al-Tabbaa A, Antonaci P, Baera C, Bajare D, et al. A review of self-healing concrete for damage management of structures. *Adv Mater Interfaces*. 2018;5(17):1800074.
 242. Zhang K, Tang C-S, Jiang N-J, Pan X-H, Liu B, Wang Y-J, et al. Microbial-induced carbonate precipitation (MICP) technology: a review on the fundamentals and engineering applications. *Environ Earth Sci*. 2023;82(9):229.
 243. Dranseike D, Cui Y, Ling AS, Donat F, Bernhard S, Bernero M, et al. Dual carbon sequestration with photosynthetic living materials. *Nat Commun*. 2025;16(1):3832.
 244. Lee S, Park J-H, Kwak D, Cho K. Coral mineralization inspired CaCO₃ deposition via CO₂ sequestration from the atmosphere. *Cryst Growth Des*. 2010;10(2):851–55.
 245. Castro-Alonso MJ, Montañez-Hernandez LE, Sanchez-Muñoz MA, Macias Franco MR, Narayanasamy R, Balagurusamy N. Microbially induced calcium carbonate precipitation (MICP) and its potential in bioconcrete: microbiological and molecular concepts. *Front Mater*. 2019;6:126.
 246. Ma Y, Yi S, Wang M. Biomimetic mineralization for carbon capture and sequestration. *Carbon Capture Sci Technol*. 2024;13:100257.
 247. Deng H, Du H, Li K, Zhang Y, Lee KH, Zheng B, et al. Towards negative carbon footprint: carbon sequestration enabled manufacturing of coral-inspired tough structural composites. *npj Adv Manuf*. 2025;2(1):1.
 248. Gleizer S, Bar-On YM, Ben-Nissan R, Milo R. Engineering microbes to produce fuel, commodities, and food from CO₂. *Cell Rep Phys Sci*. 2020;1(10):100223.
 249. De Muynck W, Verbeken K, De Belie N, Verstraete W. Influence of urea and calcium dosage on the effectiveness of bacterially induced carbonate precipitation on limestone. *Ecol Eng*. 2010;36(2):99–111.
 250. Qian C, Wang A, Wang X. Advances of soil improvement with bio-grouting. *Rock Soil Mech*. 2015;36(6):1537–48.
 251. Torres-Aravena ÁE, Duarte-Nass C, Azócar L, Mella-Herrera R, Rivas M, Jeison D. Can microbially induced calcite precipitation (MICP) through a ureolytic pathway be successfully applied for removing heavy metals from wastewaters? *Crystals*. 2018;8(11):438.
 252. Rajasekar A, Wilkinson S, Moy CKS. MICP as a potential sustainable technique to treat or entrap contaminants in the natural environment: a review. *Environ Sci Ecotechnol*. 2021;6:100096.
 253. Zúñiga-Barra H, Pardo-Vásquez C, Velastegui E, Martínez-Ruano JA, Rivas M, Jeison D. Sustainable biocementation of mine tailings: reduction of urea requirements through bicarbonate-based MICP. *Environ Technol Innov*. 2025;39:104255.
 254. Gagg CR. Cement and concrete as an engineering material: an historic appraisal and case study analysis. *Eng Fail Anal*. 2014;40:114–40.
 255. Coffetti D, Crotti E, Gazzaniga G, Carrara M, Pastore T, Coppola L. Pathways towards sustainable concrete. *Cem Concr Res*. 2022;154:106718.
 256. Zhang W, Zheng Q, Ashour A, Han B. Self-healing cement concrete composites for resilient infrastructures: a review. *Compos B Eng*. 2020;189:107892.
 257. De Rooij M, Tittelboom KV, Belie ND, Schlangen E. Self-healing phenomena in cement-based materials: State-of-the-art Report of RILEM Technical Committee. Berlin: Springer; 2013.
 258. Termkhajornkit P, Nawa T, Yamashiro Y, Saito T. Self-healing ability of fly ash–cement systems. *Cem Concr Compos*. 2009;31(3):195–203.
 259. Sahmaran M, Yildirim G, Erdem TK. Self-healing capability of cementitious composites incorporating different supplementary cementitious materials. *Cem Concr Compos*. 2013;35(1):89–101.
 260. Hilloulin B, Van Tittelboom K, Gruyaert E, De Belie N, Loukili A. Design of polymeric capsules for self-healing concrete. *Cem Concr Compos*. 2015;55:298–307.
 261. White SR, Sottos NR, Geubelle PH, Moore JS, Kessler MR, Sriram SR, et al. Autonomic healing of polymer composites. *Nature*. 2001;409(6822):794–97.

262. Jonkers HM, Thijssen A, Muyzer G, Copuroglu O, Schlangen E. Application of bacteria as self-healing agent for the development of sustainable concrete. *Ecol Eng.* 2010;36(2):230–35.
263. Wu Y, Li H, Li Y. Biomineralization induced by cells of *Sporosarcina pasteurii*: mechanisms, applications and challenges. *Microorganisms.* 2021;9(11):2396.
264. Xu J, Yao W. Multiscale mechanical quantification of self-healing concrete incorporating non-ureolytic bacteria-based healing agent. *Cem Concr Res.* 2014;64:1–10.
265. Wang JY, Soens H, Verstraete W, De Belie N. Self-healing concrete by use of microencapsulated bacterial spores. *Cem Concr Res.* 2014;56:139–52.
266. Achal V, Pan X, Özyurt N. Improved strength and durability of fly ash-amended concrete by microbial calcite precipitation. *Ecol Eng.* 2011;37(4):554–59.
267. Overpeck JT. The challenge of hot drought. *Nature.* 2013;503(7476):350–51.
268. Zheng Y, Bai H, Huang Z, Tian X, Nie F-Q, Zhao Y, et al. Directional water collection on wetted spider silk. *Nature.* 2010;463(7281):640–43.
269. Bai H, Ju J, Sun R, Chen Y, Zheng Y, Jiang L. Controlled fabrication and water collection ability of bioinspired artificial spider silks. *Adv Mater.* 2011;32(23):3708–11.
270. Venkatesan H, Chen J, Liu H, Liu W, Hu J. A spider-capture-silk-like Fiber with extremely high-volume directional water collection. *Adv Funct Mater.* 2020;30(30):2002437.
271. Chen W, Guo Z. Hierarchical fibers for water collection inspired by spider silk. *Nanoscale.* 2019;11(33):15448–63.
272. Bai H, Ju J, Zheng Y, Jiang L. Functional fibers with unique wettability inspired by spider silks. *Adv Mater.* 2012;24(20):2786–91.
273. Russell SJ, Norvig P. *Artificial intelligence: a modern approach.* London: Pearson; 2016.
274. Wang H, Fu T, Du Y, Gao W, Huang K, Liu Z, et al. Scientific discovery in the age of artificial intelligence. *Nature.* 2023;620(7972):47–60.
275. Jordan MI, Mitchell TM. Machine learning: trends, perspectives, and prospects. *Science.* 2015;349(6245):255–60.
276. Butler KT, Davies DW, Cartwright H, Isayev O, Walsh A. Machine learning for molecular and materials science. *Nature.* 2018;559(7715):547–55.
277. Yang KK, Wu Z, Arnold FH. Machine-learning-guided directed evolution for protein engineering. *Nat Methods.* 2019;16(8):687–94.
278. Baek M, Dimaio F, Anishchenko I, Dauparas J, Ovchinnikov S, Lee GR, et al. Accurate prediction of protein structures and interactions using a three-track neural network. *Science.* 2021;373(6557):871–76.
279. Jumper J, Evans R, Pritzel A, Green T, Figurnov M, Ronneberger O, et al. Highly accurate protein structure prediction with AlphaFold. *Nature.* 2021;596(7873):583–89.
280. Greener JG, Kandathil SM, Moffat L, Jones DT. A guide to machine learning for biologists. *Nat Rev Mol Cell Biol.* 2022;23(1):40–55.
281. Goldenberg SL, Nir G, Salcudean SE. A new era: artificial intelligence and machine learning in prostate cancer. *Nat Rev Urol.* 2019;16(7):391–403.
282. Gagne Ii DJ, Haupt SE, Nychka DW, Thompson G. Interpretable deep learning for spatial analysis of severe hailstorms. *Mon Weather Rev.* 2019;147(8):2827–45.
283. Degraeve J, Felici F, Buchli J, Neunert M, Tracey B, Carpanese F, et al. Magnetic control of tokamak plasmas through deep reinforcement learning. *Nature.* 2022;602(7897):414–19.
284. Flecker AS, Shi Q, Almeida RM, Angarita H, Gomes-Selman JM, Garcia-Villacorta R, et al. Reducing adverse impacts of Amazon hydropower expansion. *Science.* 2022;375(6582):753–60.
285. Roussel R, Gonzalez-Aguilera JP, Kim Y-K, Wisniewski E, Liu W, Piot P, et al. Turn-key constrained parameter space exploration for particle accelerators using Bayesian active learning. *Nat Commun.* 2021;12(1):5612.
286. Guo K, Yang Z, Yu C-H, Buehler MJ. Artificial intelligence and machine learning in design of mechanical materials. *Mater Horiz.* 2021;8(4):1153–72.
287. Batra R, Song L, Ramprasad R. Emerging materials intelligence ecosystems propelled by machine learning. *Nat Rev Mater.* 2021;6(8):655–78.
288. Bank RPD. *The RCSB Protein Data Bank.* 2025 [cited 2025 Feb 18]. Available from: <https://www.rcsb.org/>
289. Steinegger M, Mirdita M, Söding J. Protein-level assembly increases protein sequence recovery from metagenomic samples manyfold. *Nat Methods.* 2019;16(7):603–6.
290. Kuhlman B, Dantas G, Ireton GC, Varani G, Stoddard BL, Baker D. Design of a novel globular protein fold with atomic-level accuracy. *Science.* 2003;302(5649):1364–68.
291. Tunyasuvunakool K, Adler J, Wu Z, Green T, Zielinski M, Židek A, et al. Highly accurate protein structure prediction for the human proteome. *Nature.* 2021;596(7873):590–96.
292. Huang P-S, Boyken SE, Baker D. The coming of age of de novo protein design. *Nature.* 2016;537(7620):320–27.
293. Notin P, Rollins N, Gal Y, Sander C, Marks D. Machine learning for functional protein design. *Nat Biotechnol.* 2024;42(2):216–28.
294. Jiang L, Althoff EA, Clemente FR, Doyle L, Röthlisberger D, Zanghellini A, et al. De novo computational design of retroaldol enzymes. *Science.* 2008;319(5868):1387–91.
295. Bale JB, Gonen S, Liu Y, Sheffler W, Ellis D, Thomas C, et al. Accurate design of megadalton-scale two-component icosahedral protein complexes. *Science.* 2016;353(6297):389–94.
296. Arakawa K, Kono N, Malay AD, Tateishi A, Ifuku N, Masunaga H, et al. 1000 spider silkomes: linking sequences to silk physical properties. *Sci Adv.* 2022;8(41):eabo6043.
297. Huang W, Ebrahimi D, Dinjaski N, Tarakanova A, Buehler MJ, Wong JY, et al. Synergistic integration of experimental and simulation approaches for the de novo design of silk-based materials. *Acc Chem Res.* 2017;50(4):866–76.
298. Lin S, Ryu S, Tokareva O, Gronau G, Jacobsen MM, Huang W, et al. Predictive modelling-based design and experiments for synthesis and spinning of bioinspired silk fibres. *Nat Commun.* 2015;6(1):6892.
299. Pandey A, Chen W, Keten S. Sequence-based data-constrained deep learning framework to predict spider dragline mechanical properties. *Commun Mater.* 2024;5(1):83.
300. Shi Y-X, Zhu Y-J, Qian Z-G, Xia X-X. Artificial spider silk materials: from molecular design, mesoscopic assembly, to macroscopic performances. *Adv Funct Mater.* 2025;35:2412793.

301. Lu W, Kaplan DL, Buehler MJ. Generative modeling, design, and analysis of spider silk protein sequences for enhanced mechanical properties. *Adv Funct Mater.* 2024;34(11):2311324.
302. Chen L, Tran H, Batra R, Kim C, Ramprasad R. Machine learning models for the lattice thermal conductivity prediction of inorganic materials. *Comput Mater Sci.* 2019;170:109155.
303. Xie T, Grossman JC. Crystal graph convolutional neural networks for an accurate and interpretable prediction of material properties. *Phys Rev Lett.* 2018;120(14):145301.
304. Xiao H, Li R, Shi X, Chen Y, Zhu L, Chen X, et al. An invertible, invariant crystal representation for inverse design of solid-state materials using generative deep learning. *Nat Commun.* 2023;14(1):7027.
305. Shen SC, Khare E, Lee NA, Saad MK, Kaplan DL, Buehler MJ. Computational design and manufacturing of sustainable materials through first-principles and materiomics. *Chem Rev.* 2023;123(5):2242–75.
306. Park K, Song C, Park J, Ryu S. Multi-objective Bayesian optimization for the design of nacre-inspired composites: optimizing and understanding biomimetics through AI. *Mater Horiz.* 2023;10(10):4329–43.
307. Zeni C, Pinsler R, Zügner D, Fowler A, Horton M, Fu X, et al. A generative model for inorganic materials design. *Nature.* 2025;639:624–32.
308. Sanchez-Lengeling B, Aspuru-Guzik A. Inverse molecular design using machine learning: generative models for matter engineering. *Science.* 2018;361(6400):360–65.
309. Yang Z, Yu C-H, Buehler MJ. Deep learning model to predict complex stress and strain fields in hierarchical composites. *Sci Adv.* 2021;7(15):eabd7416.
310. Louie SG, Chan Y-H, Da Jornada FH, Li Z, Qiu DY. Discovering and understanding materials through computation. *Nat Mater.* 2021;20(6):728–35.
311. Ning Z, Gong X, Comin R, Walters G, Fan F, Voznyy O, et al. Quantum-dot-in-perovskite solids. *Nature.* 2015;523(7560):324–28.
312. Bertolini S, Balbuena PB. Buildup of the solid electrolyte interphase on lithium-metal anodes: reactive molecular dynamics study. *J Phys Chem C.* 2018;122(20):10783–91.
313. Jaiswal AK, Srivastava R, Pandey P, Bandyopadhyay P. Microscopic picture of water-ethylene glycol interaction near a model DNA by computer simulation: concentration dependence, structure, and localized thermodynamics. *PLoS ONE.* 2018;13(11):e0206359.
314. Senior AW, Evans R, Jumper J, Kirkpatrick J, Sifre L, Green T, et al. Improved protein structure prediction using potentials from deep learning. *Nature.* 2020;577(7792):706–10.
315. Rudraraju S, Salvi A, Garikipati K, Waas AM. Predictions of crack propagation using a variational multiscale approach and its application to fracture in laminated fiber reinforced composites. *Compos Struct.* 2012;94(11):3336–46.
316. Vasudevan RK, Choudhary K, Mehta A, Smith R, Kusne G, Tavazza F, et al. Materials science in the artificial intelligence age: high-throughput library generation, machine learning, and a pathway from correlations to the underpinning physics. *MRS Commun.* 2019;9(3):821–38.
317. Wang H-C, Botti S, Marques MAL. Predicting stable crystalline compounds using chemical similarity. *npj Comput Mater.* 2021;7(1):12.
318. Jain A, Ong SP, Hautier G, Chen W, Richards WD, Dacek S, et al. Commentary: the Materials Project: a materials genome approach to accelerating materials innovation. *APL Mater.* 2013;1(1):011002.
319. Schmidt J, Wang H-C, Cerqueira TFT, Botti S, Marques MAL. A dataset of 175k stable and metastable materials calculated with the PBEsol and SCAN functionals. *Sci Data.* 2022;9(1):64.
320. Schmidt J, Hoffmann N, Wang H-C, Borlido P, Carriço PJMA, Cerqueira TFT, et al. Large-scale machine-learning-assisted exploration of the whole materials space. *arXiv.2210.00579.* 2022.
321. Jiao R, Huang W, Lin P, Han J, Chen P, Lu Y, et al. Crystal structure prediction by joint equivariant diffusion. *Adv Neural Inf Process Syst.* 2023;36:17464–97.
322. Lu W, Lee NA, Buehler MJ. Modeling and design of heterogeneous hierarchical bioinspired spider web structures using deep learning and additive manufacturing. *Proc Natl Acad Sci.* 2023;120(31):e2305273120.
323. Chiang Y-H, Tseng B-Y, Wang J-P, Chen Y-W, Tung C-C, Yu C-H, et al. Generating three-dimensional bioinspired microstructures using transformer-based generative adversarial network. *J Mater. Res. Technol.* 2023;27:6117–34.
324. Sarvestani HY, Singh A, Ashrafi B. Bridging nature and technology: a perspective on role of machine learning in bioinspired ceramics. *Adv Eng Mater.* 2024:2400792.
325. Wu Z, Pan H, Huang P, Tang J, She W. Biomimetic mechanical robust cement-resin composites with machine learning-assisted gradient hierarchical structures. *Adv Mater.* 2024;36(35):2405183.
326. Ibrahim S, D'Andrea L, Gastaldi D, Rivolta MW, Vena P. Machine learning approaches for the design of biomechanically compatible bone tissue engineering scaffolds. *Comput Meth Appl Mech Eng.* 2024;423:116842.
327. D'Andrea L, Gabrieli R, Milano L, Magagnin L, Cet AD, Alidoost D, et al. Elastic and failure characterization of hydroxyapatite TPMS scaffolds using a combined approach of ultrasound, compression tests and micro-CT based numerical models. *Acta Mater.* 2025;287:120776.
328. Buehler MJ. A computational building block approach towards multiscale architected materials analysis and design with application to hierarchical metal metamaterials. *Modell Simul Mater Sci Eng.* 2023;31(5):054001.
329. Maurizi M, Gao C, Berto F. Inverse design of truss lattice materials with superior buckling resistance. *npj Comput Mater.* 2022;8(1):247.
330. Buehler MJ. Generating 3D architected nature-inspired materials and granular media using diffusion models based on language cues. *Oxf Open Mater Sci.* 2022;2(1):itac010.
331. Shen SC-y, Buehler MJ. Nature-inspired architected materials using unsupervised deep learning. *Comms Eng.* 2022;1(1):37.
332. Gu GX, Chen C-T, Richmond DJ, Buehler MJ. Bioinspired hierarchical composite design using machine learning: simulation, additive manufacturing, and experiment. *Mater Horiz.* 2018;5:939–45.
333. Gu GX, Chen C-T, Buehler MJ. De novo composite design based on machine learning algorithm. *Extreme Mech Lett.* 2018;18:19–28.
334. Buehler MJ. Predicting mechanical fields near cracks using a progressive transformer diffusion model and exploration

- of generalization capacity. *J Mater Res.* 2023;38(5):1317–31.
335. Lew AJ, Buehler MJ. Single-shot forward and inverse hierarchical architected materials design for nonlinear mechanical properties using an attention-diffusion model. *Mater Today.* 2023;64:10–20.
336. Open AI, Achiam J, Adler S, Agarwal S, Ahmad L, Akkaya I, et al. Gpt-4 technical report. arXiv: 2303.08774 2023.
337. Buehler MJ. MechGPT, a language-based strategy for mechanics and materials modeling that connects knowledge across scales, disciplines, and modalities. *Appl Mech Rev.* 2024;76(2):021001.
338. Luu RK, Buehler MJ. BioinspiredLLM: conversational large language model for the mechanics of biological and bio-inspired materials. *Adv Sci.* 2024;11(10):2306724.
339. Friederich P, Häse F, Proppe J, Aspuru-Guzik A. Machine-learned potentials for next-generation matter simulations. *Nat Mater.* 2021;20(6):750–61.
340. Jiang Y, Li X, Luo H, Yin S, Kaynak O. Quo vadis artificial intelligence? *Discov Artif Intell.* 2022;2(1):4.

How to cite this article: Fu Q, Baino F, Saiz E, Bai H, Mauro JC. Nature-inspired hierarchical materials. *J Am Ceram Soc.* 2025;108:e70156. <https://doi.org/10.1111/jace.70156>